

EFFECT OF MICROWAVE ASSISTED EXTRACTION ON THE PHENOLIC  
CONTENT AND PROFILE OF DIFFERENT SORGHUM PHENOTYPES

A Thesis

by

KAITLYN MARIE DUKE

Submitted to the Office of Graduate and Professional Studies of  
Texas A&M University  
in partial fulfillment of the requirements for the degree of

MASTER OF SCIENCE

Chair of Committee,  
Committee Members,

Joseph Awika  
Bhimu Patil  
Steve Talcott  
Audrey Girard

Head of Department,

Bhimu Patil

May 2021

Major Subject: Food Science and Technology

Copyright 2021 Kaitlyn Marie Duke

## ABSTRACT

Sorghum contains diverse bioactive compounds, particularly polyphenolics, which have been associated with various health benefits. These compounds are concentrated in the bran fraction that is lost during milling. The goal of this study was to establish how microwave assisted extraction (MAE) affects the extractability and profile of polyphenolics from the bran of different sorghum phenotypes. Sorghums with different grain and plant colors were selected and the effect of microwave energy on the phenolic profile (UPLC-MSMS), and content (HPLC, UV-vis spectroscopy) was evaluated. Conventional extraction (1% HCl in MeOH/2 hr.) was used as a control.

Extractable phenolic content increased 3.4-3.5X for the white pericarp sorghums, while non-tannin pigmented sorghums only increased to 1.1-1.2X versus the control. The greatest increase in extractable phenolic content from MAE treatment increased was in the red tannin sorghum phenotype (3.8X). Similar trends occurred in the antioxidant capacity of each phenotype. White and tannin phenotype antioxidant capacity increased 3.4-3.6X, while non-tannin pigmented sorghums increased 1.3-2.2X versus control treatment.

Phenolic profile and structural identification paralleled the findings from the UV-vis analysis, and helped elucidate changes in phenolic content due to MAE. Phenolic acid content increased (1.6-11X) in MAE extracts in phenotypes which contained low levels of free phenolic acids, while the phenolic content in phenotypes high in free phenolic acids decreased. Free phenolic acids that were easily extracted in the

conventional method, were rapidly degraded under MAE. In contrast, bound phenolic acids attached to the cell wall material were released by MAE and contributed to the significant increases in quantified phenolic acid content in MAE extracts. Flavanone aglycones seemed to be more resistant to degradation than the glycosides under MAE. Following MAE, anthocyanidins were detected in the tannin sample; this was likely due to the oxidative depolymerization of the condensed tannins under MAE conditions.

MAE is potentially a useful and efficient tool for extracting polyphenolic compounds from sorghum bran. Further understanding of how phenotype plays a role in the extraction efficiency of MAE can help improve extraction efficiency of specific polyphenolic compounds.

## DEDICATION

To my parents, Dr. Tammy Kay Rooney Duke and Mr. Steven Alan Duke, for your constant support, advice, and encouragement throughout my studies.

To my dear husband Luke, for your patience and reassurance, especially during these last few months.

To my son, your upcoming arrival has been a source of motivation for completing this manuscript.

I love you all.

## ACKNOWLEDGEMENTS

I would like to especially thank my committee chair, Dr. Joseph Awika, for giving me this opportunity to research and learn in the Cereal Quality Lab. His support, mentoring, patience, and guidance throughout this time has impacted me greatly. Additionally, I would like to thank my committee members, Dr. Stephen Talcott, Dr. Bhimu Patil, and Dr. Audrey Girard for their guidance, support, and advice throughout my graduate studies.

Thank you also to my colleagues in the Cereal Quality Lab—Dr. Tadesse Teferra, Dr. Shreeya Ravisankar, Dr. Julia Brantsen, Suliman Althwab, Fariha Irshad, Cyprian Syuenda, Kathryn Le Mere, and Gabrielle Scott. Their support, encouragement, knowledge, and friendship developed me as a researcher, collaborator, and person. My time here would not have been the same without them.

## CONTRIBUTORS AND FUNDING SOURCES

### **Contributors**

This work was supervised by a thesis committee consisting of Dr. Joseph Awika [advisor] of the Department of Soil and Crop Sciences, Dr. Bhimu Patil of the Department of Horticultural Sciences, Dr. Steve Talcott of the Department of Nutrition and Food Science, and Dr. Audrey Girard of the Department of Soil and Crop Sciences.

Dr. Shreeya Ravisankar contributed to Chapter 4 by identifying ferulic acid compounds and helping to identify the structure of methylcyanidin.

All work conducted for the thesis was completed by the student independently.

### **Funding Sources**

This work was partially supported by the USDA National Institute for Food and Agriculture Hatch Project No. 1003810.

## NOMENCLATURE

MAE	Microwave-Assisted Extraction
HPLC	High Performance Liquid Chromatography
UPLC	Ultra Performance Liquid Chromatography
UV-Vis	Ultraviolet-Visible Spectroscopy
Acidified methanol	1% HCl in methanol
GAE	Gallic Acid Equivalents
TE	Trolox Equivalents
W/T	White Pericarp, Tan Secondary Plant Color
W/P	White Pericarp, Purple Secondary Plant Color
R/T	Red Pericarp, Tan Secondary Plant Color
R/P	Red Pericarp, Purple Secondary Plant Color
Y/P	Lemon Yellow Pericarp, Purple Secondary Plant Color

## TABLE OF CONTENTS

	Page
ABSTRACT .....	ii
DEDICATION .....	iv
ACKNOWLEDGEMENTS .....	v
CONTRIBUTORS AND FUNDING SOURCES.....	vi
NOMENCLATURE.....	vii
TABLE OF CONTENTS .....	viii
LIST OF FIGURES.....	x
LIST OF TABLES .....	xii
CHAPTER I INTRODUCTION .....	1
CHAPTER II LITERATURE REVIEW .....	3
Sorghum Grain Structure and Diversity.....	3
Sorghum Polyphenols .....	4
Phenolic Acids.....	4
Monomeric Flavonoids.....	6
Polymeric Flavonoids.....	10
Benefits of Polyphenols to Human Health.....	11
Microwave Assisted Extraction .....	13
CHAPTER III MATERIALS AND METHODS.....	14
Materials.....	14
Sorghum Bran.....	14
Chemicals and Reagents.....	15
Methods.....	15
Extraction Methods .....	15
UV-Vis Analysis .....	16
RP-HPLC Analysis for Polyphenol Profile.....	19
UPLC-MSMS Analysis for Polyphenol Identification .....	19



Statistical Analysis .....	21
<b>CHAPTER IV EFFECT OF MICROWAVE ASSISTED EXTRACTION (MAE) ON THE PHENOLIC PROFILE OF SORGHUM BRAN .....</b>	<b>22</b>
Introduction .....	22
Identification of Phenolic Acid Peaks .....	30
Identification of Flavanone Peaks .....	36
Identification of Flavone Peaks .....	39
Identification of Anthocyanin Peaks .....	41
Effect of MAE on Phenolic Profile .....	45
Quantification of Major Phenolic Peaks .....	46
Quantification of Phenolic Acids .....	47
Quantification of Flavanones .....	49
Quantification of Flavones .....	50
Quantification of 3-Deoxyanthocyanins .....	51
Conclusion.....	52
<b>CHAPTER V EFFECT OF MICROWAVE ASSISTED EXTRACTION (MAE) ON EXTRACTABLE PHENOLICS AND ANTIOXIDANT CAPACITY OF SORGHUM BRANS.....</b>	<b>54</b>
Sorghum Phenotypes Selected for Analysis .....	54
Effect of MAE on Total Extractable Phenolic Content.....	54
Effect of MAE on Antioxidant Capacity.....	59
Conclusion.....	64
<b>CHAPTER VI CONCLUSIONS .....</b>	<b>65</b>
<b>REFERENCES .....</b>	<b>68</b>

## LIST OF FIGURES

	Page
Figure 1. Phenolic acids common to sorghum grain and their structures .....	5
Figure 2. Monomeric flavonoids common in sorghum grain and their structures .....	7
Figure 3. Structure of anthocyanins compared to 3-deoxyanthocyanins found in sorghum grain .....	9
Figure 4. Structure of condensed tannins in sorghum grain.....	10
Figure 5. Phenolic profiles of control and MAE treatments for ATx635/RTx436 (W/T) sorghum bran. Numbers are associated with phenolic compounds identified in Table 2. Profile at 280 and 325 nm. ....	23
Figure 6. Phenolic profiles of control and MAE treatments for 17CS5417 (W/P) sorghum bran. Numbers are associated with phenolic compounds identified in Table 2. Profile at 280 and 325 nm. ....	24
Figure 7. Phenolic profiles of control and MAE treatments for NK8830 (R/T) sorghum bran. Numbers are associated with phenolic compounds identified in Table 2. Profile at 280 and 325 nm. ....	25
Figure 8. Phenolic profiles of control and MAE treatments for ATx2911 (R/P) sorghum bran. Numbers are associated with phenolic compounds identified in Table 2. Profile at 280 and 325 nm. ....	26
Figure 9. Phenolic profiles of control and MAE treatments for ATx642/RO6321 (Y/P) sorghum bran. Numbers are associated with phenolic compounds identified in Table 2. Profile at 280 and 325 nm. ....	27
Figure 10. Structures of the phenolic acid derivatives identified in sorghum phenotypes. ....	35
Figure 11. Structures of proposed flavanone derivatives identified in sorghum phenotypes. ....	38
Figure 12. Structures of proposed flavone derivatives identified in sorghum phenotypes .....	40
Figure 13. Structures of proposed anthocyanidin derivatives identified in sorghum phenotypes .....	44

Figure 14. Total extractable phenolics for control and MAE treated ATx635/RTx436 (W/T) sorghum bran. Error bars = $\pm$ Standard Deviation (n=3) *a-c: denotes statistical significance (p<0.05).....	55
Figure 15. Total extractable phenolics for control and MAE treated 17CS5417 (W/P) sorghum bran. Error bars = $\pm$ Standard Deviation (n=3) *a-b: denotes statistical significance (p<0.05).....	56
Figure 16. Total extractable phenolics for control and MAE treated NK8830 (R/T) sorghum bran. Error bars = $\pm$ Standard Deviation (n=3) *a-c: denotes statistical significance (p<0.05).....	56
Figure 17. Total extractable phenolics for control and MAE treated ATx2911 (R/P) sorghum bran. Error bars = $\pm$ Standard Deviation (n=3) *a-b: denotes statistical significance (p<0.05).....	57
Figure 18. Total extractable phenolics for control and MAE treated ATx642/RO6321 (Y/P) sorghum bran. Error bars = $\pm$ Standard Deviation (n=3) *a-c: denotes statistical significance (p<0.05).....	57
Figure 19. Antioxidant capacity measured by trolox equivalents (TE) for control and MAE treated ATx 635/RTx436 sorghum bran. Error bars = $\pm$ Standard Deviation (n=3) *a-c: denotes statistical significance (p<0.05).....	61
Figure 20. Antioxidant capacity measured by trolox equivalents (TE) for control and MAE treated 17CS5417 sorghum bran. Error bars = $\pm$ Standard Deviation (n=3) *a-c: denotes statistical significance (p<0.05).....	62
Figure 21. Antioxidant capacity measured by trolox equivalents (TE) for control and MAE treated NK8830 sorghum bran. Error bars = $\pm$ Standard Deviation (n=3) *a-c: denotes statistical significance (p<0.05).....	62
Figure 22. Antioxidant capacity measured by trolox equivalents (TE) for control and MAE treated ATx2911 sorghum bran. Error bars = $\pm$ Standard Deviation (n=3) *a-c: denotes statistical significance (p<0.05).....	63
Figure 23. Antioxidant capacity measured by trolox equivalents (TE) for control and MAE treated ATx642/RO6321 sorghum bran. Error bars = $\pm$ Standard Deviation (n=3) *a-c: denotes statistical significance (p<0.05).....	63

## LIST OF TABLES

	Page
Table 1. Sorghum variety and phenotype abbreviations. ....	22
Table 2. Proposed identities of phenolic compounds found in sorghum phenotypes. ....	28
Table 3. Proposed identities of phenolic acid compounds found in sorghum phenotypes. ....	34
Table 4. Proposed identities of flavanone compounds found in sorghum phenotypes. ....	38
Table 5. Proposed identities of flavone compounds found in sorghum phenotypes. ....	40
Table 6. Proposed identities of anthocyanin compounds found in sorghum phenotypes. ....	44
Table 7. Quantified phenolic content by compound type and treatment. ....	47
Table 8. Quantified phenolic content between treatments. ....	47
Table 9. Quantification of detected phenolic acid derivatives in each phenotype. ....	49
Table 10. Quantification of detected flavanones in each phenotype. ....	50
Table 11. Quantification of detected flavones in each phenotype. ....	51
Table 12. Quantification of detected anthocyanidins in each phenotype by treatment. ....	52
Table 13. Sorghum phenotypes used in this study and notations. ....	54

## CHAPTER I

### INTRODUCTION

Sorghum has grown in popularity as a health food as it is rich in nutrients, is a source of health-beneficial compounds, and is gluten free. In 2018, 58.8 million tonnes of sorghum was produced worldwide. With 2.04 million hectares of farmland devoted to sorghum production and an average yield of 4.5 tonnes of grain per hectare, the United States produced 9.2 million tonnes of sorghum grain or approximately 15% of worldwide production (USDA, 2019). Sorghum ranks fifth worldwide in terms of cereal grain production (USDA, 2019). Uses for sorghum vary depending on the location of production. The United States primarily uses sorghum for livestock feed and ethanol production, whereas drought prone countries depend on sorghum grain for nourishment where maize, rice, and wheat often fail (Zhao and Dahlberg, 2019).

The rise of sorghum in American culture can be attributed to research linking its bioactive compounds, such as polyphenolics, to protection against chronic illness. Other benefits include reduced starch digestibility due to extensive crosslinking of kafirin proteins within the endosperm during wet cooking, which lowers the glycemic index (Simnadis et al., 2016; Teferra et al., 2019). Sorghum is also naturally gluten free, is safe for celiac patients, and has been incorporated into a variety of products which are marketed to be gluten free.

Sorghum grain varieties offer a wide range of polyphenolic compounds concentrated primarily in the bran. Polyphenolics such as phenolic acids and flavonoids

have been shown to have high antioxidant capacity and chemopreventative potential (Yang, 2009; Yang et al., 2012). However, each sorghum variety offers a different amount and type of phenolic compounds. Understanding how grain color, plant color, and other genetic factors impact the phenolic components of this important cereal grain is vital to utilizing it to the greatest extent. Unfortunately, many of the beneficial phenolic compounds in the grain are lost with the bran when the grain is decorticated to meet consumer acceptance. Finding a way to extract these compounds efficiently and effectively from the bran waste stream can add value to a byproduct that is otherwise lost.

The overall goal of this study is to understand how microwave assisted extraction (MAE) affects the extractability of phenolics from different types of sorghum. Previous research from the Texas A&M Cereal Quality Lab has shown that MAE more efficiently extracts 3-deoxyanthocyanin pigments from black sorghum compared to the control extraction method (Herrman et al., 2020). Therefore, the hypothesis is that the polyphenolic compounds in sorghum can be efficiently extracted using MAE.

The objectives of this study are to:

1. Identify changes in phenolic profile of different sorghum varieties due to microwave assisted extraction;
2. Determine the effect of MAE on extraction efficiency of sorghum polyphenols.

## CHAPTER II

### LITERATURE REVIEW

#### **Sorghum Grain Structure and Diversity**

Sorghum (*Sorghum bicolor*) is a diverse grain that serves many functions worldwide. In some arid parts of Africa, it is grown as a primary source of food, whereas in other parts of the world it functions primarily as animal feed and used for ethanol production. Many different types of sorghum are grown in the United States today; silage sorghum is grown for animal feed, biomass sorghum for ethanol production, and grain sorghum is grown for human and animal consumption (Borden, 2011; Dykes et al., 2011). The focus of the rest of this literature review is on grain sorghum.

Sorghum grain contains three distinct parts, the bran (pericarp and testa), the endosperm, and the germ. The bran contains non-starch polysaccharides, is rich in polyphenolic compounds, and genotypes with a pigmented testa contain condensed tannins. The endosperm is made up of mostly starch, proteins, some polyphenolics, and micronutrients such as vitamins and minerals. The germ contains lipids, proteins, minerals, and lipid soluble vitamins.

Grain sorghum comes in a number of different varieties, which impacts the nutritive benefits of the sorghum. Genetic factors predetermine many qualities of the grain including pericarp color and thickness, grain hardness, and secondary plant color (Dykes, 2008; Dykes et al., 2009). The pericarp color, easily identified as the color of the grain, can be either white, yellow, or red and can vary greatly in intensity. Black

sorghum is actually a red sorghum which turns black when in direct sunlight (Dykes, 2008; Dykes et al., 2009). Pericarp thickness determines whether starch is present in the pericarp; thick pericarps contain starch granules whereas thin pericarps do not. Grain hardness has been associated with higher concentrations of phenolic acids (Chiremba et al., 2012b; Girard and Awika, 2018). Secondary plant color is another important genetic factor that influences the properties of the grain. There are two secondary plant colors, tan or purple, which also impact the phenolic profile of the sorghum grain (Dykes, 2008).

### **Sorghum Polyphenols**

Sorghum grain contains a wide range of polyphenolic compounds. The type and prevalence of different compounds depends on sorghum genotypes, and is also influenced by the growing environment (Dykes et al., 2005; Przybylska-Balcerek et al., 2019). The most common phenolic compounds that occur in sorghum grain are phenolic acids (e.g. benzoic and cinnamic acids and their derivatives), monomeric flavonoids (e.g. flavones, flavanones, 3-deoxyanthocyanins), and polymeric flavonoids (condensed tannins).

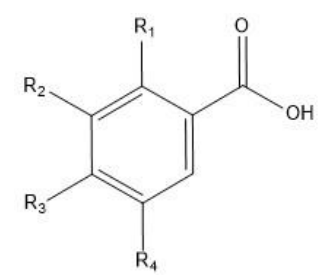
#### *Phenolic Acids*

Two classes of phenolic acids are found in all sorghum grain: benzoic and cinnamic acids (Dykes, 2008; Zhao and Dahlberg, 2019). Phenolic acids are the most abundant and most characterized group of phenolic compounds found in cereal grains. They are found throughout the grain, in the pericarp as well as the endosperm; usually



bound to the cell wall polysaccharides (Dykes et al., 2011). While both cinnamic and benzoic acids are prevalent, cinnamic acid derivatives are the most abundant (Awika, 2014; Girard and Awika, 2018). Benzoic acids derivatives common to sorghum include gallic, vanillic, p-hydroxybenzoic, protocatechuic acids, and syringic acids (Girard and Awika, 2018). Caffeic, p-coumeric, ferulic, and sinapinic acids are common cinnamic acids in grain sorghum (Girard and Awika, 2018). **Figure 1** contains a list of common benzoic and cinnamic acids and their structures found in sorghum grain.

<b>Phenolic Acids</b>				
a. Benzoic Acid Derivatives				
Acid	R <sub>1</sub>	R <sub>2</sub>	R <sub>3</sub>	R <sub>4</sub>
Gallic	H	OH	OH	OH
p-Hydroxybenzoic	H	H	OH	H
Vanillic	H	H	OH	OCH <sub>3</sub>
Protocatechuric	H	H	OH	OH
Syringic	H	OCH <sub>3</sub>	OH	OCH <sub>3</sub>
b. Cinnamic Acid Derivatives				
Acid	R <sub>1</sub>	R <sub>2</sub>	R <sub>3</sub>	R <sub>4</sub>
p-Coumaric	H	H	OH	H
Caffeic	H	OH	OH	H
Ferulic	H	H	OH	OCH <sub>3</sub>
Sinapinic	H	OCH <sub>3</sub>	OH	OCH <sub>3</sub>



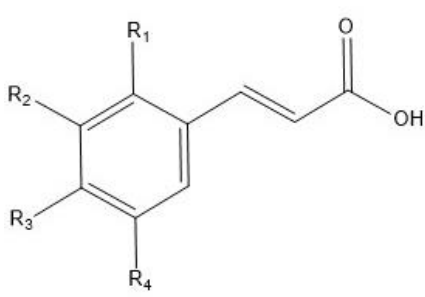


**Figure 1. Phenolic acids common to sorghum grain and their structures**

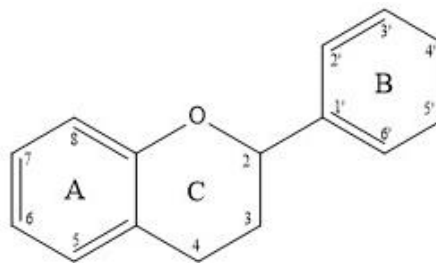
Phenolic acids are structural components of cell wall material in cereal grains and are commonly bound via esterification to hemicelluloses. Ferulic acid derivatives are the most abundant phenolic acid in cell wall material followed by p-coumaric acid (Chiremba et al., 2012b). Higher concentrations of phenolic acids typically occur in harder grains due to a greater amount of crosslinking between ferulic acid and cell wall polysaccharides (Chiremba et al., 2012b; Girard and Awika, 2018). As it is extremely uncommon that unbound free forms of these phenolics exist in cereal grains, bound forms have a unique nutritional benefit (Svensson et al., 2010). Bound phenolics, which are unable to be absorbed directly in the upper gastrointestinal, are broken down by the gut microbiota and provide a slow release of bioactive compounds to the body (Awika et al., 2018; Mateo Anson et al., 2011).

### *Monomeric Flavonoids*

Another large group of polyphenolics found in sorghum are the monomeric flavonoids. Flavonoids are compounds that contain a C<sub>6</sub>-C<sub>3</sub>-C<sub>6</sub> skeleton which includes three rings joined through a three-carbon linkage (**Figure 2a**). Flavonoids are located primarily in the pericarp of all cereal grains, and sorghum has the largest assortment of flavonoids reported in literature (Dykes and Rooney, 2007). Common flavonoids in sorghum include flavones, flavanones, and 3-deoxyanthocyanins. **Figure 2** contains a list of common sorghum flavonoids and their structures.

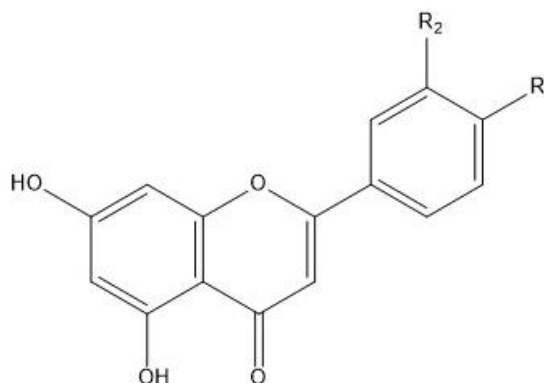
## Monomeric Flavonoids

### a. Flavonoid Skeleton



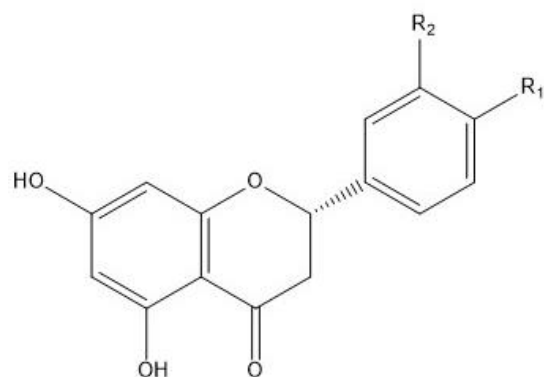
### b. Flavones

Flavone	R <sub>1</sub>	R <sub>2</sub>
Apigenin	H	OH
Luteolin	OH	OH
Derivatives	substitution of OH, with OCH <sub>3</sub> or O-glycosides on C <sub>5</sub> or C <sub>7</sub>	



### c. Flavanones

Flavanone	R <sub>1</sub>	R <sub>2</sub>
Eriodictyol	OH	OH
Naringenin	H	OH
Derivatives	substitution of OH, with OCH <sub>3</sub> or O-glycosides on C <sub>5</sub> or C <sub>7</sub>	



### d. 3-Deoxyanthocyanins

Flavone	R <sub>1</sub>	R <sub>2</sub>
Apigeninidin	H	OH
Luteolinidin	OH	OH
Derivatives	Substitution of OH, with OCH <sub>3</sub> or O-glycosides on C <sub>5</sub> or C <sub>7</sub>	

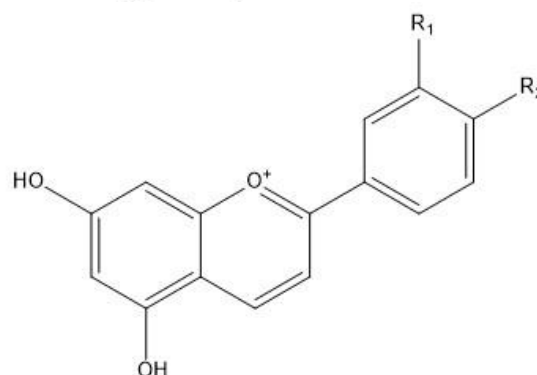


Figure 2. Monomeric flavonoids common in sorghum grain and their structures

## **Flavones**

In sorghum, flavones commonly exist primarily as aglycones and as O-linked glycosides (**Figure 2b**) (Awika, 2011; Dykes et al., 2011; Xiong et al., 2019). The most common flavones in sorghum are apigenin and luteolin and their derivatives. White sorghums, as well as lemon yellow and red varieties with a tan plan secondary color tend to have the highest concentrations of flavones (Dykes et al., 2011, 2009). Sorghums with tan secondary colors also tend to have higher concentrations of apigenin based flavonoids, whereas purple secondary colored sorghums contain higher levels of luteolin based flavonoids (Awika, 2014). Glycosidic forms, while naturally present, are unstable in the presence of acid- leading to the rapid hydrolysis of the O-glycoside from flavones (Awika, 2011; Dykes et al., 2011; Svensson et al., 2010; Xiong et al., 2019).

## **Flavanones**

Flavanones (**Figure 2c**), are fairly uncommon in cereal grains, however some sorghum varieties seem to be an exception as they can contain over 2000 µg/g of these compounds (Awika, 2014; Dykes et al., 2011). Unlike flavones, flavanones are completely absent in white sorghum varieties. Instead they are found in yellow and red pericarp sorghum varieties (Dykes, 2008; Dykes et al., 2011). Eriodictyol and naringenin, as well as their glycoside derivatives, have both been identified in yellow sorghums while only the latter have been recorded in red varieties (Dykes, 2008; Dykes et al., 2011, 2009).

### 3-Deoxyanthocyanins

Another class of flavonoids found in sorghum are the 3-deoxyanthocyanins (**Figure 2d**). These compounds contribute to the color of the sorghum grain. These 3-deoxyanthocyanins are a special class of anthocyanins found only in sorghum. They specifically lack a substitute at the C3 position of the C-ring which increases their stability to pH change, heat, and oxidizing agents compared to regular anthocyanins (Mazza and Brouillard, 1987; Ojwang and Awika, 2008; Sweeny and Iacobucci, 1983; Liyi Yang et al., 2014). This makes the 3-deoxyanthocyanins valuable as natural food colorants. The 3-deoxyanthocyanins are most commonly found in yellow and red sorghums, as well as plants with a purple secondary color (Dykes, 2008). The most common 3-deoxyanthocyanins to sorghum are apigenindin and luteolinidin (Awika et al., 2005b; Pale et al., 1997). The structure of anthocyanins and 3-deoxyanthocyanins is shown in **Figure 3**.

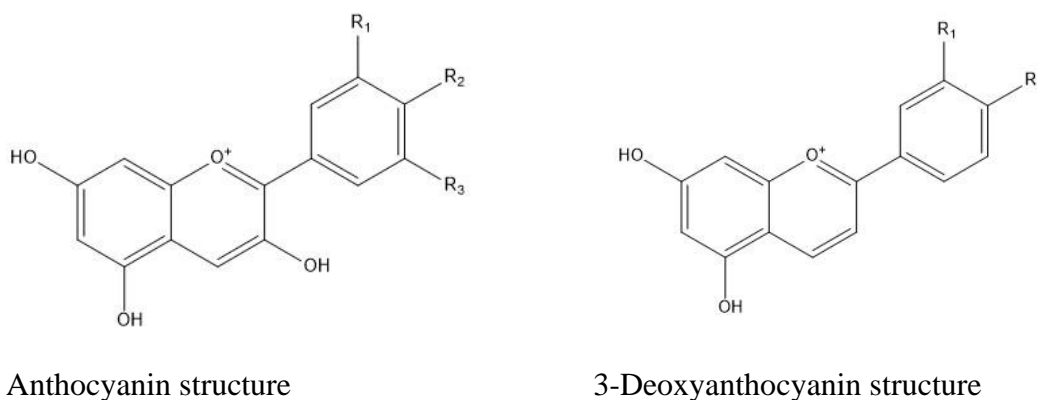


**Figure 3. Structure of anthocyanins compared to 3-deoxyanthocyanins found in sorghum grain**

### *Polymeric Flavonoids*

Tannins are one of the most researched classes of polyphenolics as they are common to many different plants such as tea leaves, grapes, legumes, and cacao and serve as natural deterrents to pests and molds (Combs, 2016; Wu et al., 2012). Sorghum contains highly polymerized forms of tannin known as condensed tannins (**Figure 4**).

Condensed tannins are polymers of flavonoids consisting of flavan-3-ols, 3-

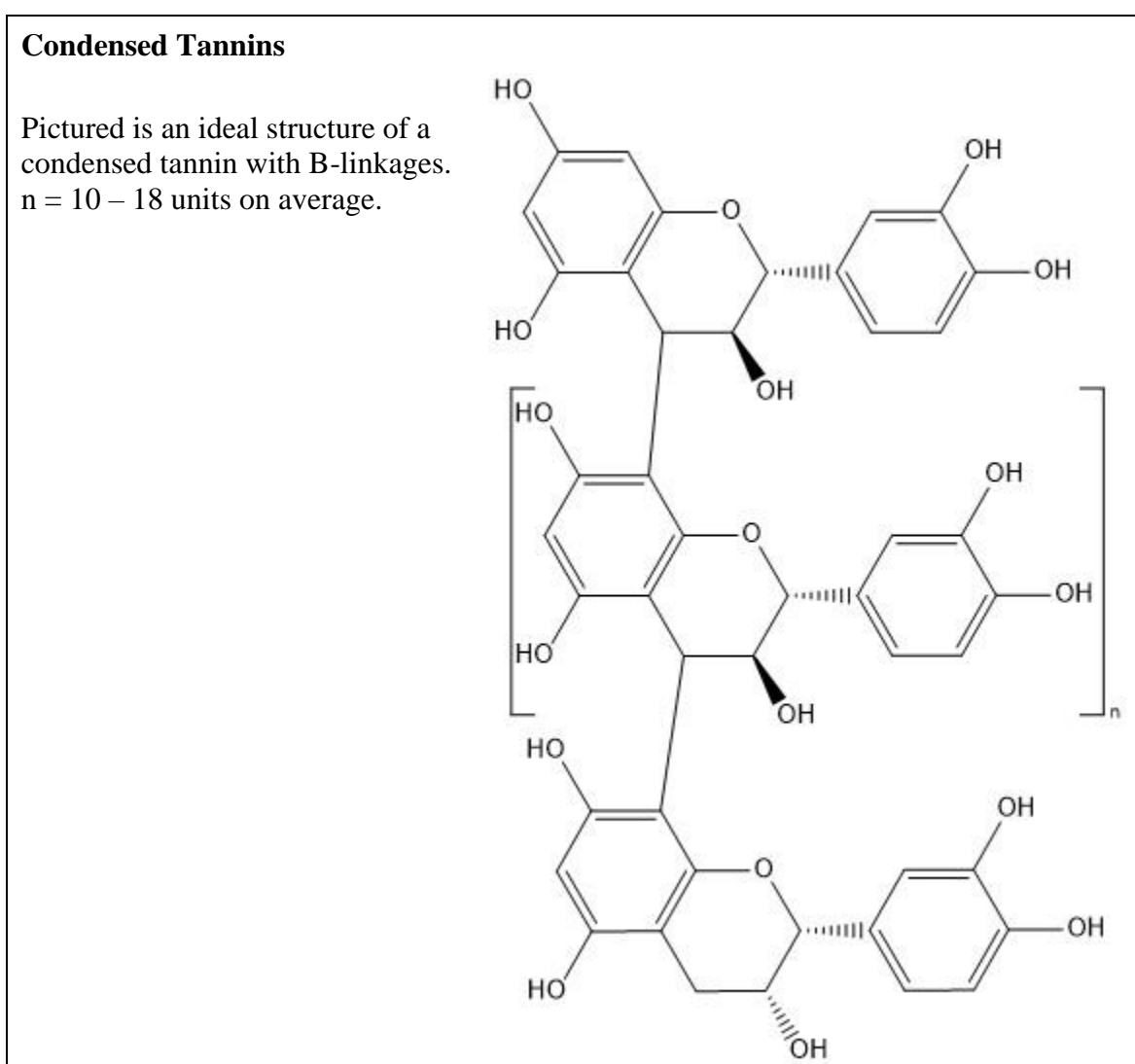


**Figure 4. Structure of condensed tannins in sorghum grain**

deoxyanthocyanins, and flavanones with an average degree of polymerization of approximately 20 (Girard and Awika, 2018). The biggest concern in regards to condensed tannins is how they impact the nutritional value of sorghum. Tannins are known to bind to proteins thereby reducing protein digestibility, as well as complex with key micronutrients such as iron and zinc potentially decreasing their bioavailability (Awika, 2014). The tannin content in sorghum is highly variable, and sorghum varieties can be divided into different types based on tannin content: Type I sorghum has very low amounts of tannins (0 - 1.5 mg CAE/g) and are generally considered tannin free. Type II has a moderate amount of tannins (6.4 – 15.5 mg CAE/g) which are located within the testa. Type III sorghum has the highest amount of tannins (11 – 50 mg CAE/g) found within the testa, cell walls, and pericarp (C.F. Earp, 1981; Dykes and Rooney, 2006). Type III sorghum has the greatest impact on sorghum digestibility (Awika, 2014; Xiong et al., 2019).

### **Benefits of Polyphenols to Human Health**

The health benefits of polyphenols have been well documented. The common assumption is that a higher antioxidant capacity equates to an increased health benefit; however, this is not necessarily the case. Instead, the composition of antioxidant compounds and how they interact with each other *in vivo* affect the potential benefit of a food (Awika, 2014).

Sorghum has been shown to have a higher *in vitro* antioxidant capacity than other cereal grains (Dykes et al., 2005). The classes of unique polyphenols common to

sorghum, rather than the high radical scavenging ability, is what makes sorghum a valuable source of health benefits. Bound phenolic acids, such as ferulic acid bound to the cell wall polysaccharides in sorghum, are broken down by the gut microbiota and provide a slow release of bioactive compounds to the body (Awika et al., 2018; Mateo Anson et al., 2011). Flavones, such as apigenin, have shown to have anti-inflammatory benefits *in vitro*, and chemopreventative properties *in vivo* (Agah et al., 2017; L. Yang et al., 2014; Yang, 2009; Yang et al., 2015). Flavanones, have been shown to have chemopreventative properties when exposed to colonocytes in young adult mice, as well as reduce ovarian cancer cell (A27801AP and PTX-10) proliferation *in vitro* (Dia et al., 2016; Yang et al., 2015). Condensed tannins are shown to lower glycemic response through  $\alpha$ -amylase inhibition, as well as survive digestion until the small intestine *in vivo* (Links et al., 2016, 2015). In human studies, whole grain sorghum has been observed to improve glycemic response and increase satiety, act as an antioxidant by increasing polyphenol plasma levels and decreasing protein carbonyl levels as an indicator of oxidative stress, and reduce inflammation in patients with chronic kidney disease (Anunciação et al., 2018; Khan et al., 2015; Lopes et al., 2018; Stefoska-Needham et al., 2017, 2016).

Furthermore, the polyphenolics in sorghum are concentrated in the bran, which makes up about 10% of the grain by weight. Levels of phenolics have been measured to be about 5 times higher in the bran alone than with the whole grain (Awika et al., 2005a). Efficiently extracting polyphenolics from the sorghum bran waste stream is an



opportunity to enrich products with bioactive compounds that would otherwise be lost. Microwave assisted extraction (MAE) holds potential in this application.

### **Microwave Assisted Extraction**

Microwave assisted extraction (MAE) offers many advantages over conventional extraction techniques. These include solvent to sample ratios, extraction time, and higher yield (Beehmohun et al., 2007; Chiremba et al., 2012a; Herrman, 2016). Furthermore, the higher pressures and temperatures reached with MAE are more conducive for cell wall breakdown and subsequent release of bound phenolic compounds that cannot otherwise be extracted.

MAE has shown to be an effective tool in extracting phenolic compounds from mango peel, carob bark, emblic fruit, açai, ginger, and pomegranate peel (Aliaño-González et al., 2020; Kaderides et al., 2019; Li et al., 2019; Pal and Jadeja, 2020; Pham and Quoc, 2020; Quiles-Carrillo et al., 2019). These studies all report equal, or significantly higher phenolic yields than conventional or alternative extraction methods. MAE has also been used successfully to extract pectin from sweet lemon peel (Rahmani et al., 2020). Previous research completed in our lab shows that MAE more efficiently extracts 3-deoxyanthocyanin pigments from black sorghum compared to the control extraction method (Herrman et al., 2020). Therefore, MAE should be a valuable tool to increase the extraction of polyphenolic compounds concentrated in sorghum bran.

## CHAPTER III

### MATERIALS AND METHODS

#### **Materials**

##### *Sorghum Bran*

Five varieties of sorghum grain were chosen based on pericarp color and secondary plant color to represent diverse phenolic profiles of sorghum. These samples include 2 white, 2 red, and 1 lemon yellow seeded sorghums with tan and purple secondary plant colors. White varieties included ATx635/RTx436, tan plant (College Station, TX; 2018) and 17CS5417, purple plant (College Station, TX; 2017). Red varieties were NK8830, tan plant (2016), and Tx2911, purple plant (College Station, TX; 2016). The lemon yellow variety was ATx642/RO6321 (College Station, TX; 2016) and has a purple secondary plant color. Sorghum samples were stored at -20 °C until use. Prior to decortication grain samples were sealed in a plastic bag and allowed to equilibrate to room temperature.

Sorghum grain samples were decorticated using a PRL mini de-huller (Nutama Machine Co., Saskatoon, Canada) until 10% of the grain by weight was removed. The decorticated sorghum was sifted to remove grain and broken grain pieces from the bran, and each fraction was packaged and stored at -20 °C until use. The sorghum bran samples were further milled down using a UDY cyclone mill (Model 3010- 030, UDY Corporation, Fort Collins, CO) until fine enough to pass through a 1.0 mm mesh screen. The refined bran was stored until use at -20 °C.

### *Chemicals and Reagents*

Chemicals and reagents to be used in this study were either reagent or analytical grade. Gallic acid, catechin hydrate, 2,2'-azinobis (3-ethyl-benzothiazoline- 6-sulfonic acid (ABTS), caffeic acid, ferulic acid, disodium phosphate, monosodium phosphate, potassium persulfate, sodium chloride, and naringenin were obtained from Sigma (St. Louis, MO). Apigenin and luteolin were obtained from Indofine Chemical Co., Inc. (Hillsborough, NJ). Eriodictyol was obtained from ALSACHIM (Strasbourg, France). Methanol, acetonitrile, and water was LC-MS analytical grade. Hydrochloric acid, ethanolamine, Folin's reagent, and formic acid were reagent grade.

## **Methods**

### *Extraction Methods*

#### **Conventional Extraction**

Sorghum bran samples were extracted in medium centrifuge tubes on a shaker (VWR Shaker- model 3500, speed #6). Samples were shaken at 25 °C (room temperature) and 1 atm for 2 hours in acidified methanol (1% HCl in MeOH). Sample to solvent ratio was 1:10, and the moisture content of each grain was recorded. Following extraction, the samples were centrifuged for 10 minutes at 2400 g. The supernatant was recovered and stored in 15 mL centrifuge tubes at -20 °C until use.

## **MAE Extraction**

Sorghum bran samples were extracted with acidified methanol (1% HCl in MeOH) in microwave vessels with a maximum temperature of 100 °C for varying time and power. The sample (bran) to solvent (acidified methanol) ratio was 1:40, and the moisture content of each sample was recorded with a Halogen Moisture Analyzer (Mettler Toledo; Columbus, OH). Samples were microwaved at 300, 600, or 1200 W for 2, 7, or 10 minutes using a MARS-5 digestion microwave (CEM Corporation; Matthews, NC). Following microwave treatment, samples were transferred to 15 mL centrifuge tubes and centrifuged for 10 minutes at 2400 g. The supernatant was collected and stored in clean 15 mL centrifuge tubes at -20 °C until further use.

### *UV-Vis Analysis*

#### **Folin-Ciocalteu Test for Total Extractable Phenolics**

Total extractable phenolics were quantified using the modified method of Kaluza et al., 1980, as described by Dykes et al., 2005, and Barros et al., 2013. Prior to analysis the following solutions were prepared: 0.5M ethanolamine, Folin's reagent (200 mL Folin's reagent diluted to 1000 mL), and a 0.2 g/L gallic acid standard which is diluted to make standard dilutions of 0, 0.05, 0.1, 0.15, and 0.2 g/L. A standard curve was run first. A standard (0.1 mL) was added to a test tube followed by 0.9 mL of the ethanolamine solution. The Folin's reagent (0.4 mL) was added last, after which the solution was mixed and allowed to sit for 20 minutes prior to being read. This was repeated for each standard. After a standard curve was created with an  $R^2$  value of at

least 0.99 the sorghum samples were run in the same way the standards were. Sorghum samples extracted through conventional and MAE were used.

Samples were analyzed on a spectrophotometer (Shimadzu UV 2450, Shimadzu Scientific Instruments North America, Columbia, MD) at 600 nm. After the absorbance values were collected, the gallic acid equivalents (GAE) for each sample were calculated with the following equation:

$$\frac{abs - y}{m} \times v_o \div v \div (d \times (1 - MC)) = \mu g \text{ GAE} / g \text{ sample, db}$$

<i>abs</i> :	absorbance at 600 nm	<i>v<sub>o</sub></i> :	mL used for extraction
<i>y</i> :	y intercept on standard curve	<i>v</i> :	mL sample used for analysis
<i>m</i> :	slope on standard curve	<i>d</i> :	weight of sample used for extraction
<i>MC</i> :	moisture content of sample		

### **Trolox Equivalent Test for Antioxidant Capacity**

The method used is similar to Awika, 2003. Before analysis the following solutions were made: phosphate buffer solution (PBS) at pH 7.4 (405 mL 0.2 M Na<sub>2</sub>HPO<sub>4</sub> added to 95 mL 0.2 NaH<sub>2</sub>PO<sub>4</sub>, to which 3.77 g of NaCl and distilled water were added to make 1L of solution), mother solution (10 mL of 8 mM 2,2'-azino-bis(3-ethylbenzothiazoline-6-sulfonic acid) (ABTS) combined with 10 mL of 3 mM K<sub>2</sub>S<sub>2</sub>O<sub>8</sub>), and a 1000 μM Trolox standard. The mother solution was prepared 12 to 24 hours before analysis while the PBS and Trolox standard were prepared just prior to analysis. A working solution containing 5 mL of the mother solution and 145 mL of the PBS was made just prior to analysis.

The standard curve was prepared first. Standard dilutions were made of the Trolox from 0  $\mu\text{M}$  to 1000  $\mu\text{M}$ , increasing by 100. To a test tube 2.9 mL of working solution was added to 0.1 mL of the Trolox standard. After shaking, it was allowed to rest for 15 minutes before being read. This was repeated for each standard. Each standard was read alongside a blank containing the working solution and methanol. A standard curve was created based on change in absorbance vs Trolox concentration. Readings were to fall between 0.1 – 1.6 and the  $R^2$  value was at least 0.995.

To each sample tube, 0.1 mL of the sample was added in addition to 2.9 mL of the workings solution. After 30 minutes the absorbance of each sample, as well as a blank that contained the sample and methanol, was measured.

Samples were analyzed on a spectrophotometer (Shimadzu UV 2450, Shimadzu Scientific Instruments North America, Columbia, MD) at 734 nm. After the absorbance values were collected, the Trolox equivalents (TE) for each sample was calculated with the following equation:

$$\frac{\Delta abs - y}{m} \div \frac{d \times (1 - MC)}{v_o \times f} = \mu mol TE/g sample, db$$

<i>abs</i> :	absorbance at 600 nm	$v_o$ :	mL used for extraction
<i>y</i> :	y intercept on standard curve	<i>f</i> :	dilution factor
<i>m</i> :	slope on standard curve	<i>d</i> :	weight of sample used for extraction
<i>MC</i> :	moisture content of sample		

### *RP-HPLC Analysis for Polyphenol Profile*

Prior to analysis, sorghum bran extract samples were passed through a 0.2  $\mu\text{M}$  PTFE membrane to filter. The method used was similar to Dykes, 2008, with some minor adjustments. Samples were run on an Agilent 1200 HPLC system (Agilent Technologies, Santa Clara, CA). The system contains a quaternary pump (with degasser), an autosampler, a column compartment, and uses a diode array detector (DAD). The column used a Zorbax Eclipse Plus C18, maintained at 40 °C with a flow rate of 1 mL/min. Solvents used were 1% formic acid in water (solvent A), and 1% formic acid in acetonitrile (solvent B). The solvent gradient, based on B, was as follows: 0-5 min 5%, 5-8 min 10%, 8-32 min 22%, 32-50 min 55%, 50-52 min 55%, 52-60 min 5%, 60-65 min 5%. 10  $\mu\text{L}$  of sample was injected. Flavanones were monitored at 280 nm, cinnamic acids at 325 nm, and flavones at 340 nm.

Peak identification was accomplished by matching elution profiles and spectra data with known standards when available.

### *UPLC-MSMS Analysis for Polyphenol Identification*

Prior to analysis, sorghum bran extract samples were passed through a 0.2  $\mu\text{M}$  PTFE membrane to filter. The used was similar to Ravisankar, 2019. Samples were run on a Waters-ACQUITY-UPLC-TQD-MS/MS system (Waters Corp., Milford, MA) equipped with a photodiode array  $e\lambda$  detector and interfaced with a mass spectrometer equipped with a tandem quadrupole (TQD) electrospray ionization (ESI) detector. Peak separation was performed with a Kinetex C18 column (100  $\times$  2.10 mm, 2.6  $\mu\text{m}$ )

(Phenomenex, Torrance, CA). Column temperature was set to 40 °C with a flow rate of 0.4 mL/min. The phases were 0.05% formic acid in UPLC grade water (solvent A), and 0.05% formic acid in UPLC grade acetonitrile (solvent B). The solvent gradient, based on percent solvent B, was as follows: 0-2 min 5%, 2-8 min 35%, 8-15 min 70%, 15-20 min 70%, 20-23 min 5%, 23-27 min 5%. Injection volume was 7 µL. Flavanones were monitored at 280 nm, phenolic acids at 325 nm, and flavones at 340 nm. The negative ion mode was used to collect all mass spectrometer data. Scanning conditions were as follows: MS scan range of 120-1000 Da. MS conditions were optimized at 3 kV for capillary voltage, and cone voltage set to 30 V. Product scans were optimized with a cone voltage of 30 V, and a collision energy between 20-40 V.

Peak identification was completed based on matching PDA profiles, peak maxima, retention profile, and mass fragment patterns from literature.

Compound quantification was achieved by interpolating peak areas based on the standard curves of the pure compounds. If pure standards were unavailable, peaks were quantified based on the closest standard available, founded on the assumption that their absorptivity is similar to the closest related standard. This procedure is similar to that of Ravisankar et al., 2018, and Ojwang et al., 2012.



### *Statistical Analysis*

Each extraction will be performed in triplicate. The data will be analyzed with JMP statistical software (version 14.1; SAS Institute; Cary, NC). One-way ANOVA was used to detect treatment effect;  $\alpha=0.05$ . Post Hoc tests (Tukey-Kramer and Fischer's LSD) were used to compare means;  $p < 0.05$ .

## CHAPTER IV

### EFFECT OF MICROWAVE ASSISTED EXTRACTION (MAE) ON THE PHENOLIC PROFILE OF SORGHUM BRAN

#### Introduction

The intent of this chapter is to identify the phenolic compounds present in each sorghum phenotype, and to understand how MAE affects the phenolic profile. **Table 1**, references the sorghum varieties and phenotypes used in this study with their phenotype code that will be used throughout this chapter. **Figures 5, 6, 7, 8, and 9** show the UPLC chromatograms of each control and MAE treated phenotype at 280 and 325 nm. The peak numbers correspond to those listed in **Table 2**, as well as **Tables 3, 4, 5, and 6**.

**Table 1. Sorghum variety and phenotype abbreviations.**

<i>Sorghum Variety</i>	<i>Pericarp Color</i>	<i>Secondary Plant Color</i>	<i>Phenotype Code</i>
ATx635/RTx436	White	Tan	W/T
17CS5417	White	Purple	W/P
NK8830	Red	Tan	R/T
ATx2911	Red	Purple	R/P
ATx642/RO6321	Lemon Yellow	Purple	Y/P

### ATx635/RTx436 (W/T)

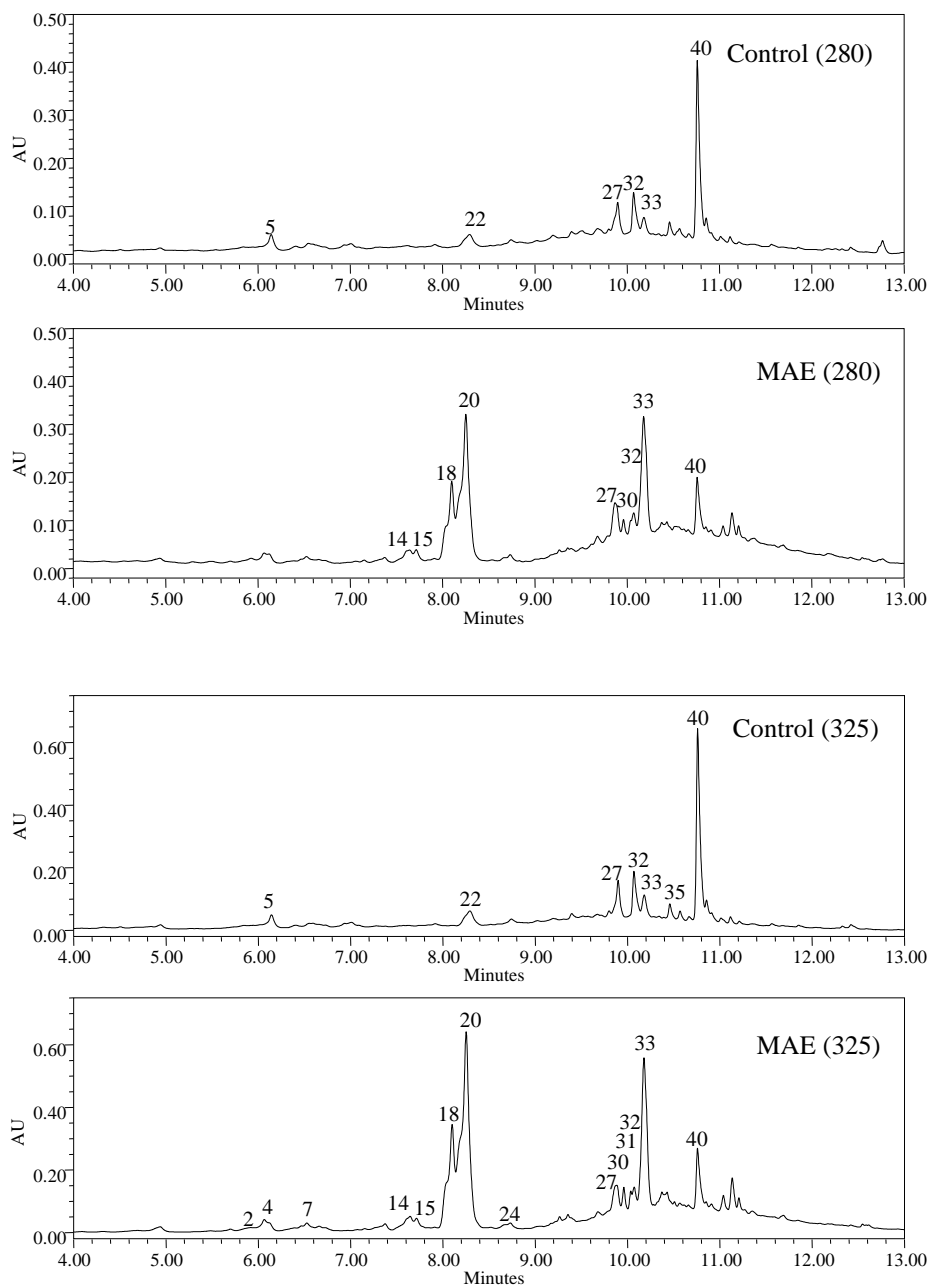


**Figure 5. Phenolic profiles of control and MAE treatments for ATx635/RTx436 (W/T) sorghum bran. Numbers are associated with phenolic compounds identified in Table 2. Profile at 280 and 325 nm.**

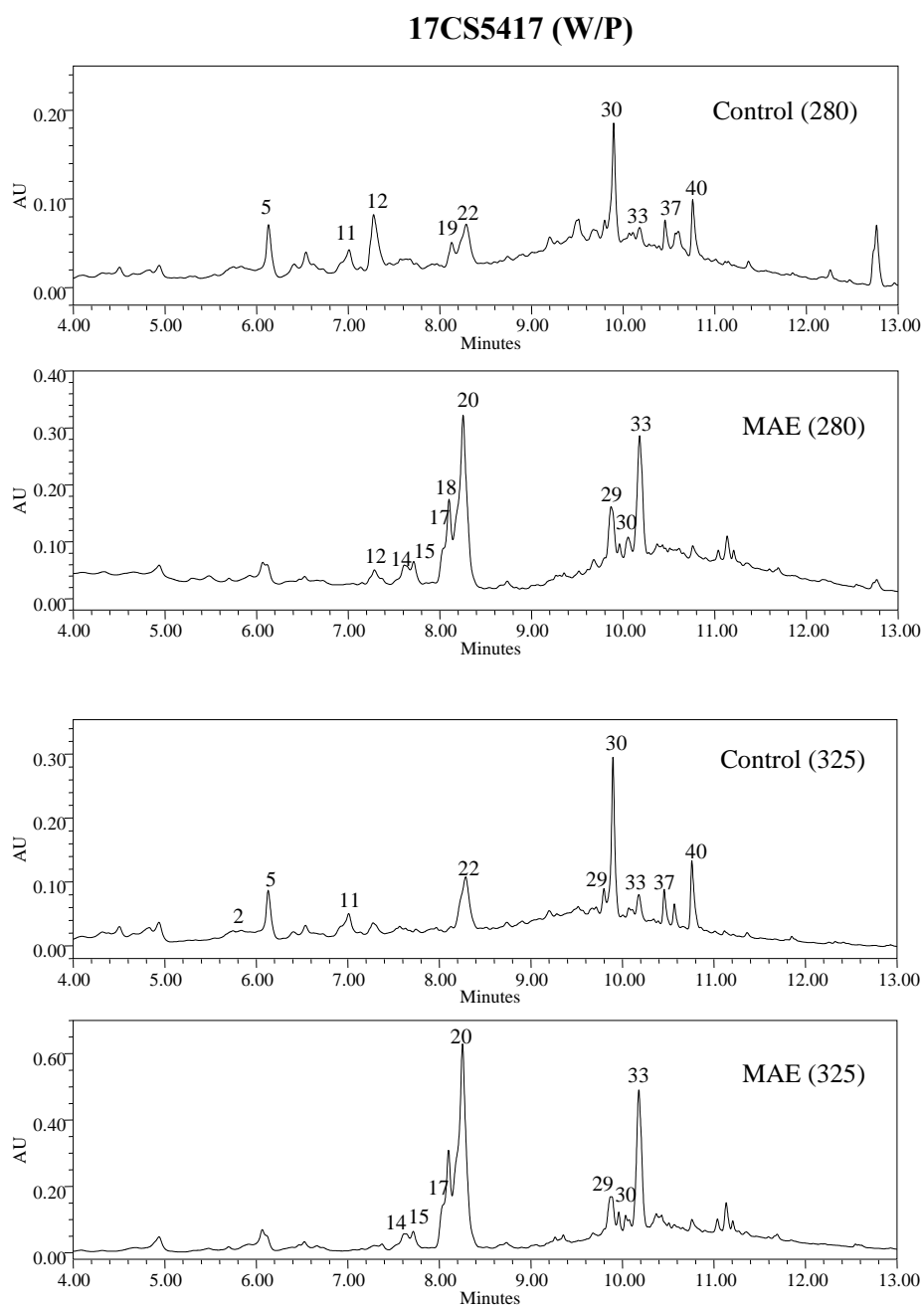


**Figure 6. Phenolic profiles of control and MAE treatments for 17CS5417 (W/P) sorghum bran. Numbers are associated with phenolic compounds identified in Table 2. Profile at 280 and 325 nm.**

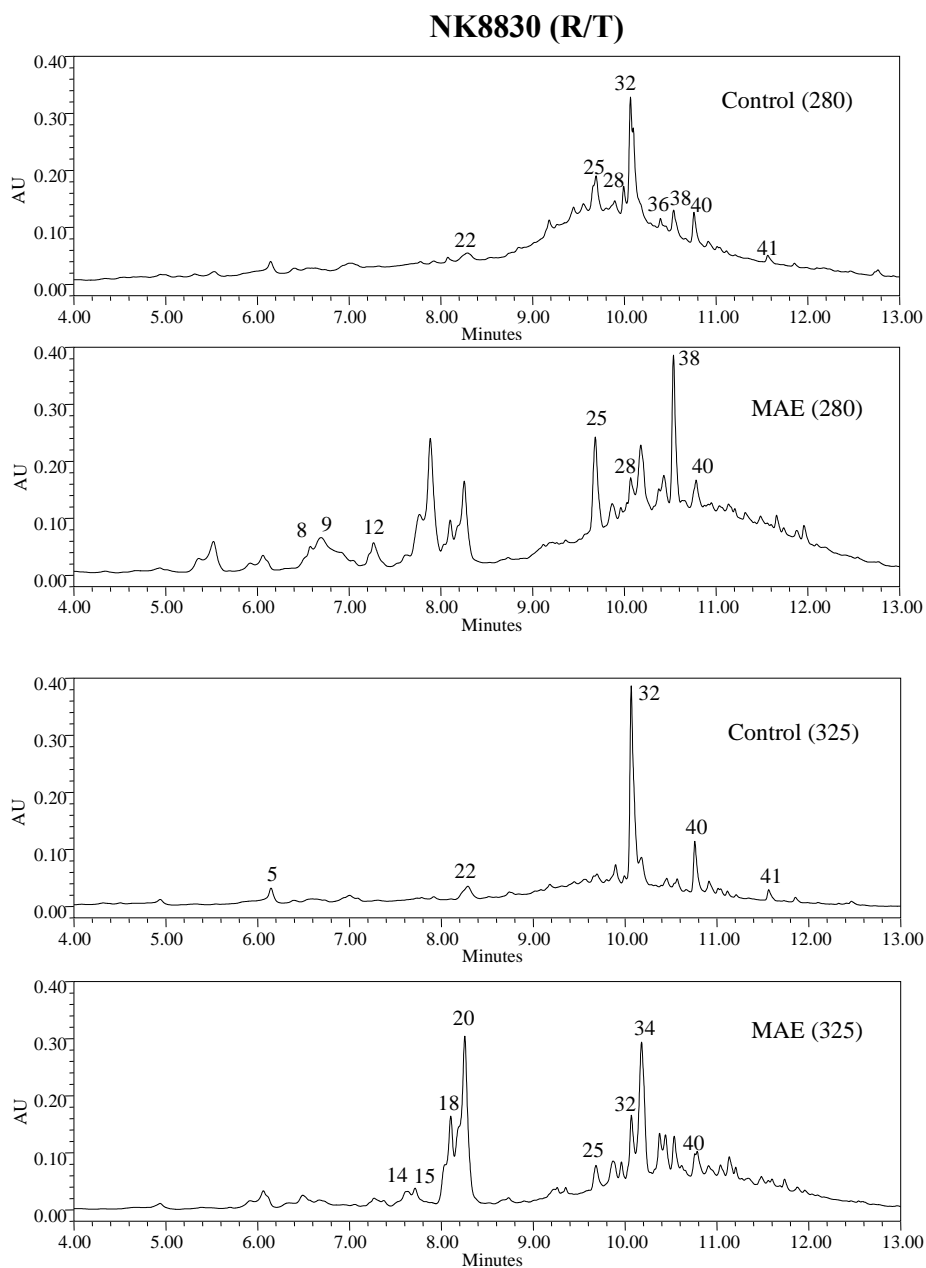


**Figure 7. Phenolic profiles of control and MAE treatments for NK8830 (R/T) sorghum bran. Numbers are associated with phenolic compounds identified in Table 2. Profile at 280 and 325 nm.**

### ATx2911 (R/P)

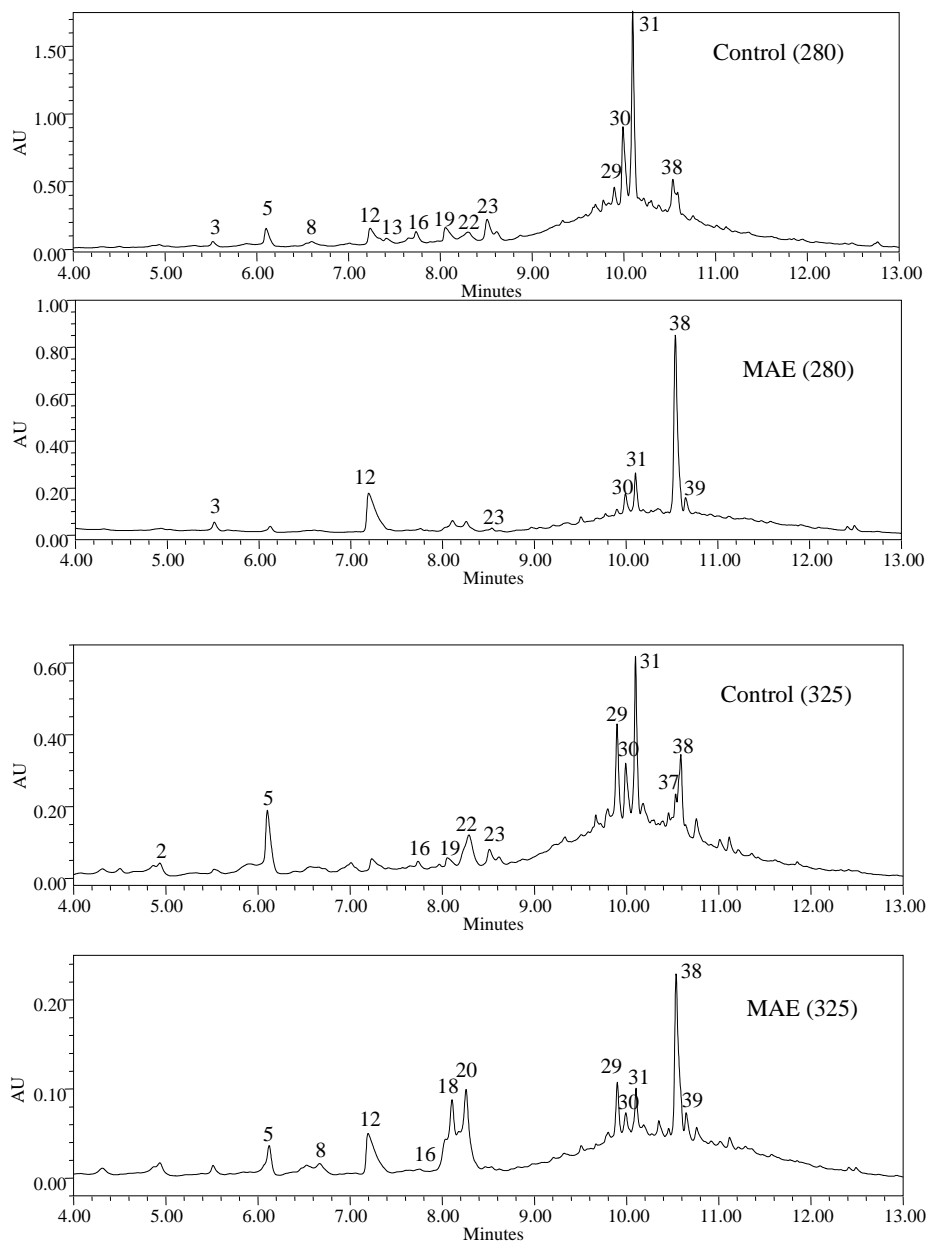


**Figure 8. Phenolic profiles of control and MAE treatments for ATx2911 (R/P) sorghum bran. Numbers are associated with phenolic compounds identified in Table 2. Profile at 280 and 325 nm.**

### ATx642/RO6321 (Y/P)

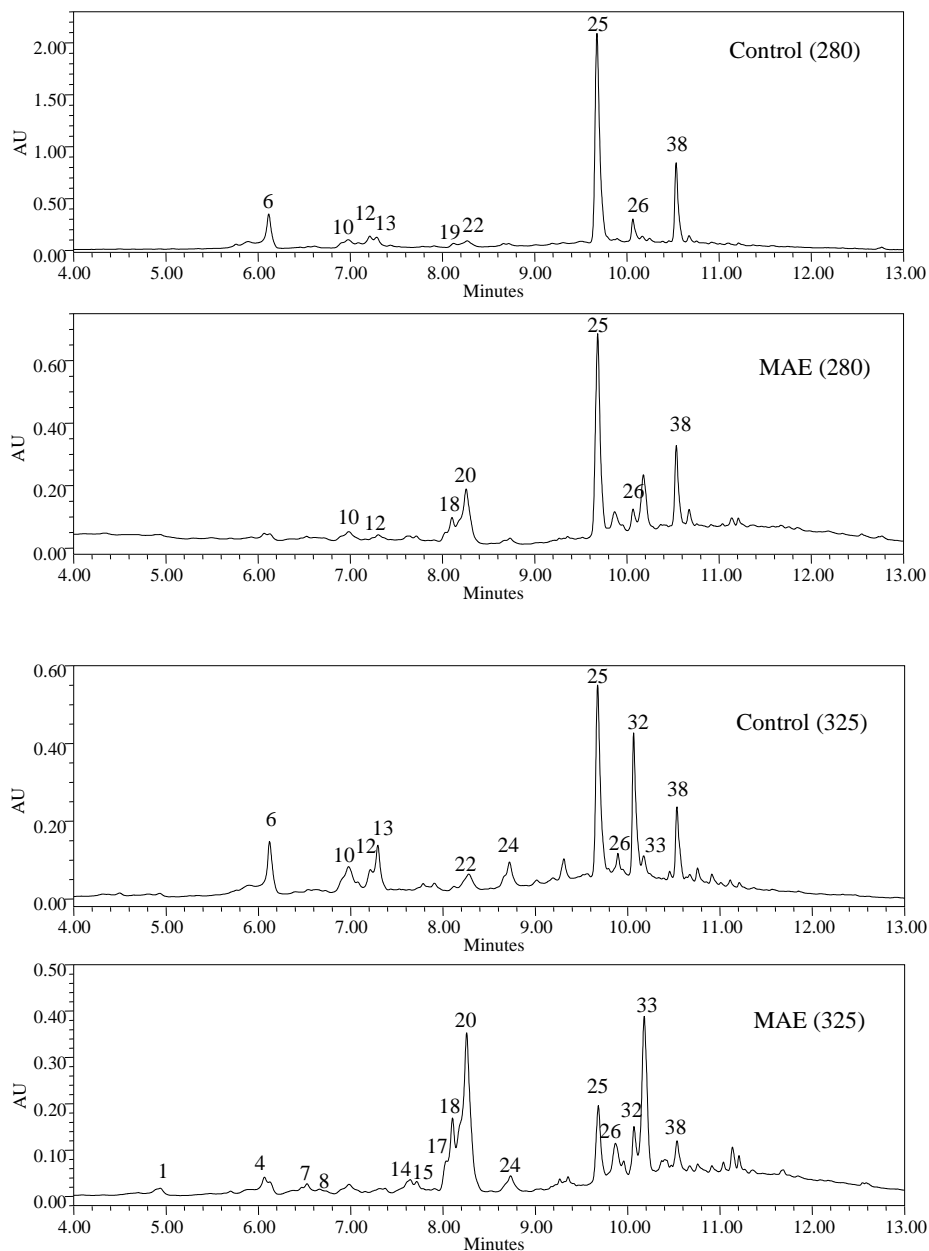


**Figure 9. Phenolic profiles of control and MAE treatments for ATx642/RO6321 (Y/P) sorghum bran. Numbers are associated with phenolic compounds identified in Table 2. Profile at 280 and 325 nm.**

**Table 2. Proposed identities of phenolic compounds found in sorghum phenotypes.**

Peak no.	Retention Time	$\lambda_{\max}$	[M-H]-	MS/MS Fragments	Proposed Identification	Sorghum Phenotype Detected													
						CTL W/T	CTL W/P	CTL R/T	CTL R/P	CTL Y/P	MAE W/T	MAE W/P	MAE R/T	MAE R/P	MAE Y/P				
1	4.93	322	253	161 (100), 148 (5)	2-O-Caffeoylglycerol														X
2	4.95	322	253	179 (17), 161 (50), 135(100)	1-O-Caffeoylglycerol		X		X		X								
3	5.52	470	417*	255 (100)	Apigeninidin-glycoside				X										
4	6.06	322	355	197 (6), 161 (100), 133 (45)	Feruloylgalactoside						X								X
5	6.10	319	468	332 (73), 135 (100), 306 (43)	N, N' -Dicafeoylspermidine	X	X	X	X									X	
6	6.13	283	449	135 (100), 287 (75), 151 (81)	Eriodictyol-glycoside					X									
7	6.53	322	325	264 (7), 179 (52), 161 (100)	Feruloyl-arabinoside						X								X
8	6.60	488	271*	179 (87), 173 (100), 131 (61)	Luteolinidin				X	X				X	X			X	X
9	6.70	521	287*	185 (100), 167 (45), 107 (40)	Cyanidin									X					
10	6.98	294	433	271 (100), 177 (73), 91 (93)	Naringenin-glycoside					X									X
11	7.02	315	355	193 (100), 133 (47)	Feruloyl-glucoside		X												
12	7.28	473	255*	213 (39), 171 (100), 69 (87)	Apigeninidin		X		X	X		X	X	X	X	X	X	X	X
13	7.42	484	285*	271 (30), 242 (100), 160 (32)	7-OMe-Luteolinidin				X	X									
14	7.64	315	309	145 (100), 119 (22), 117 (17)	Feruloyl-deoxyarabinoside						X	X	X						X
15	7.73	311	309	145 (100), 117 (51)	Feruloyl-deoxyarabinoside						X	X	X						X
16	7.74	481	836*	673 (27) 511 (100) 385 (66)	Unknown Pigment				X									X	
17	8.03	326	339	324 (96), 175 (100), 160 (62)	Feruloyl-rhamnoside							X							X
18	8.10	326	339	177 (13), 175 (100), 134 (18)	Feruloyl-rhamnoside						X	X	X	X	X	X	X	X	X
19	8.13	470	269*	226 (100), 197 (21), 144 (27)	7-OMe-Apigeninidin		X		X	X		X	X	X	X	X	X	X	X
20	8.25	326	339	177 (8), 175 (100), 160 (20)	Feruloyl-rhamnoside						X	X	X	X	X	X	X	X	X
21	8.30	477	269*	254 (10) 226 (100) 169 (30)	5-OMe-Apigeninidin				X										
22	8.31	322	193	161 (41), 134 (100), 133 (36)	Ferulic Acid	X	X	X	X	X									
23	8.52	485	283*	269 (100), 226 (85), 169 (26)	5,7 -Dimethoxyapigeninidin				X									X	
24	8.74	319	205	155 (100), 113 (16), 70 (21)	Unknown					X	X								X
25	9.68	287	287	151 (100), 135 (58), 107 (35)	Eriodictyol			X		X				X					X
26	9.87	297	333	216 (87), 203 (100)	Unknown					X									X
27	9.89	322	193	117 (100), 116 (58), 89 (15)	Unknown	X					X								
28	9.90	283	515	372 (22), 276 (38), 191 (100)	Unknown			X						X					

\* = Run in ES+ Mode



Table 2. Cont...															
Peak no.	Retention Time	$\lambda_{\max}$	[M-H]-	MS/MS Fragments	Proposed Identification	Sorghum Phenotype Detected									
						CTL W/T	CTL W/P	CTL R/T	CTL R/P	CTL Y/P	MAE W/T	MAE W/P	MAE R/T	MAE R/P	MAE Y/P
29	9.90	320	415	304 (39), 253 (100), 135 (82)	Dicaffeoylglycerol		X		X			X		X	
30	9.91	322	415	253 (54), 179 (91), 161 (100)	Dicaffeoylglycerol		X		X		X	X		X	
31	10.00	326	415	179 (35), 161 (48), 135(100)	Dicaffeoylglycerol				X		X			X	
32	10.07	347	285	133 (96),107 (65), 65 (100)	Luteolin	X		X		X	X		X	X	
33	10.17	322	285	254 (21), 175 (26), 133 (100)	Unknown	X	X			X	X	X		X	
34	10.19	322	301	287(56) 164 (100), 125 (75)	Methoxycyanidin								X		
35	10.45	315	153	150 (100), 120 (93)	Unknown	X									
36	10.46	279	657	397 (72), 209 (100)	Unknown			X							
37	10.46	315	399	163 (100), 161 (27), 119 (46)	p-coumaroyl-caffeoyl-glycerol		X		X						
38	10.55	287	271	151 (100), 119 (29),107 (18)	Naringenin			X	X	X			X	X	
39	10.66	477	655*	271 (100), 165 (44), 29 (4)	Luteolinidin derivative								X		
40	10.77	337	269	151 (69), 117 (100), 107 (93)	Apigenin	X	X	X			X		X		
41	11.56	340	515	490 (56), 125 (55), 85 (100)	Unknown			X							

\* = Run in ES+ Mode

### Identification of Phenolic Acid Peaks

Peaks 1 and 2 ( $t_R$  4.93 and 4.95 min,  $\lambda_{max} = 322$ ) had  $[M-H]^-$  at  $m/z$  253. Peak fragments had  $m/z$  at 161 ( $[M-H]^- - 92$ ) and 148 ( $[M-H]^- - 105$ ). This matches the fragmentation pattern of O-Caffeoylglycerol (**Table 3**) seen in white sorghum extracts (Ravisankar et al., 2018; Yang et al., 2012). Previous work has shown that 2-O-position elutes before 1-O-position on a reverse phase column, therefore Peaks 1 and 2 were identified as identified as 2-O-Caffeoylglycerol and 1-O-Caffeoylglycerol respectively (Ravisankar, 2019). Peak 1 was identified in the Y/P MAE treated sample. Peak 2 was identified in the control samples of the W/P and R/P phenotypes, and the MAE treated W/T phenotype (**Table 3**).

Peak 4 ( $t_R$  6.06 min,  $\lambda_{max} = 322$ ) had  $[M-H]^-$  at 355  $m/z$  (**Table 3**). Peak fragments has  $m/z$  at 197 ( $[M-H]^- - 158$ ), 161 ( $[M-H]^- - 194$ ), and 133 ( $[M-H]^- - 222$ ). The fragment peak at 161 (-194) is consistent with the loss of a ferulic acid, resulting in a hexose unit. The fragments at 161 and 133 are common breakdown products of ferulic acid. Peak 4 was identified as a feruloyl-glycoside, and upon later identification of peak 11, as feruloyl-galactoside and was detected in the W/T and Y/P phenotypes processed with MAE (**Table 3**).

Peak 5 ( $t_R$  6.10 min,  $\lambda_{max} = 319$ ) had  $[M-H]^-$  at 468  $m/z$  (**Table 3**). Peak fragments had  $m/z$  at 332 ( $[M-H]^- - 136$ ), 135 ( $[M-H]^- - 333$ ), and 306 ( $[M-H]^- - 162$ ). A loss of 136 represents the loss of a caffeoyl group, and the fragmentation pattern of 332, 135, and 306 are consistent with  $N,N'$ -Dicafeoylspermidine identified in previous literature (Kang et al., 2016; Ravisankar et al., 2018). This peak was identified in control

extracts of the W/T, W/P, and R/T phenotypes, as well as both MAE and control extracts of the R/P phenotype (**Table 3**).

Peak 7 ( $t_R$  6.53 min,  $\lambda_{max} = 322$ ) had  $[M-H]^-$  at 325 m/z (**Table 3**). Peak fragments has m/z at 264 ( $[M-H]^- - 61$ ), 179 ( $[M-H]^- - 146$ ), and 161 ( $[M-H]^- - 164$ ). The fragments at 161 and 133 are common breakdown products of ferulic acid. The fragment peak at 264 (-61) is consistent with cleavage across the arabinose ring of feruloyl-arabinoside. Peak 7 was identified as a feruloyl-arabinoside and was detected in the W/T and Y/P phenotypes processed with MAE. It has been previously identified in maize and wheat after enzymatic digestion (Malunga and Beta, 2016) (**Table 3**).

Peak 11 ( $t_R$  7.02 min,  $\lambda_{max} = 315$ ) had  $[M-H]^-$  at 355 m/z. Peak fragments has m/z at 193 ( $[M-H]^- - 162$ ), and 133 ( $[M-H]^- - 222$ ) (**Table 3**). The fragment peak at 193 is consistent with the loss of a hexose unit, resulting in a ferulic acid. The fragment at 133 is a common breakdown product of ferulic acid. Feruloyl-galactoside and feruloyl-glucoside were assigned to peaks 4, and 11 respectively as galactoside is known to elute before a glucoside on a RP column. Peak 11 was detected in the W/P phenotype control (**Table 3**).

Peak 14, and 15 ( $t_R$  7.64 and 7.73 min,  $\lambda_{max} = 315$  and 311) had  $[M-H]^-$  at m/z 309. Peak fragments had m/z at 145 ( $[M-H]^- - 164$ ), 119 ( $[M-H]^- - 190$ ), and 117 ( $[M-H]^- - 192$ ) (**Table 3**). Peak fragment at 117 is consistent with the loss of a ferulic acid, resulting in a deoxypentose unit. Peak 14 and 15 were identified as isomers of feruloyl-deoxyarabinose. Peak 14 and 15 were both identified in W/T, W/P, R/T, and Y/P phenotypes treated with MAE (**Table 3**).

Peak 17, 18, and 20 ( $t_R$  8.03, 8.10, and 8.25 min,  $\lambda_{max} = 326$ ) had  $[M-H]^-$  at  $m/z$  339. Peak fragments had  $m/z$  at 324 ( $[M-H]^- - 15$ ), 177 ( $[M-H]^- - 162$ ), 175 ( $[M-H]^- - 164$ ), 160 ( $[M-H]^- - 179$ ), and 134 ( $[M-H]^- - 205$ ) (**Table 3**). Fragments at 177 and 175 are consistent with the loss of a rhamnose unit. Fragments at 160 and 134 are common fragments of ferulic acid. Therefore peaks 17, 18, and 20 were identified as feruloyl-rhamnoside isomers. Peak 17 was detected in MAE W/P, and Y/P phenotypes. Peaks 18 and 20 were detected in all MAE phenotypes (W/T, W/P, R/T, R/P, and Y/P) (**Table 3**).

Peak 22 ( $t_R$  8.31 min,  $\lambda_{max} = 322$ ) had  $[M-H]^-$  at 193  $m/z$ . Peak fragments had  $m/z$  at 161 ( $[M-H]^- - 32$ ), 134 ( $[M-H]^- - 59$ ), and 133 ( $[M-H]^- - 60$ ) (**Table 3**). The fragmentation pattern, spectra profile, and parent mass all matched to those of known standards of ferulic acid. This peak was identified in all pericarp control samples (W/T, W/P, R/T, R/P, Y/P). This compound has been identified in white and red sorghums previously (Ravisankar, 2019; Yang, 2009) (**Table 3**).

Peak 29 ( $t_R$  9.90,  $\lambda_{max} = 320$ ) had  $[M-H]^-$  at  $m/z$  415. Peak fragments had  $m/z$  at 304 ( $[M-H]^- - 111$ ), 253 ( $[M-H]^- - 162$ ), and 135 ( $[M-H]^- - 280$ ) (**Table 3**). The peak fragment at 253 represents a caffeoylglycerol unit, and the remaining fragments are common to a caffeoylglycerol fragmentation pattern. This compound has been previously identified in white and lemon yellow sorghum, and the fragmentation pattern seen here matches that seen in literature (Ravisankar et al., 2018; Svensson et al., 2010; Yang et al., 2012). Peak 29 was identified as dicaffeoylglycerol. It was identified in the control and MAE treatments of the W/P and R/P phenotypes (**Table 3**).

Peaks 30 and 31 ( $t_R$  9.91 and 10.00 min,  $\lambda_{max} = 326$ ) had  $[M-H]^-$  at  $m/z$  415. Peak fragments had  $m/z$  at 253 ( $[M-H]^- - 162$ ), 179 ( $[M-H]^- - 236$ ), 161 ( $[M-H]^- - 254$ ), and 135 ( $[M-H]^- - 280$ ) (**Table 3**). As seen in peak 29 (**Table 3**), the peak fragment at 253 represents a caffeoylglycerol unit, and the remaining fragments are common to a caffeoylglycerol fragmentation pattern. Peak 30 was identified in control treatments of the W/P and R/P phenotypes as well as the MAE treatments of the W/T, W/P and R/P phenotypes (**Table 3**). Peak 31 was identified in the control and MAE treatments of the R/P phenotype and the MAE treatment of the W/T phenotype (**Table 3**).

Peak 37 ( $t_R$  10.46 min,  $\lambda_{max} = 315$ ) had  $[M-H]^-$  at 399  $m/z$ . Peak fragments had  $m/z$  at 163 ( $[M-H]^- - 236$ ), 161 ( $[M-H]^- - 238$ ), and 119 ( $[M-H]^- - 280$ ) (**Table 3**). This fragmentation pattern closely followed that of *p*-coumaroyl-caffeoyl-glycerol previously recorded in literature (Kang et al., 2016; Ravisankar, 2019; Svensson et al., 2010; Yang et al., 2012). Peak 37 was detected in the control treatment of the W/P and R/P phenotypes (**Table 3**).

**Table 3** contains the phenolic acid derivatives present in each corresponding phenotype and treatment. **Figure 10** shows the structures of these phenolics.

**Table 3. Proposed identities of phenolic acid compounds found in sorghum phenotypes.**

Peak no.	Retention Time	$\lambda_{\max}$	[M-H]-	MS/MS Fragments	Proposed Identification	Sorghum Phenotype Detected										
						CTL W/T	CTL W/P	CTL R/T	CTL R/P	CTL Y/P	MAE W/T	MAE W/P	MAE R/T	MAE R/P	MAE Y/P	
1	4.93	322	253	161 (100), 148 (5)	2-O-Caffeoylglycerol											X
2	4.95	322	253	179 (17), 161 (50), 135(100)	1-O-Caffeoylglycerol		X		X		X					
4	6.06	322	355	197 (6), 161 (100), 133 (45)	Feruloylgalactoside						X					X
5	6.10	319	468	332 (73), 135 (100), 306 (43)	N, N' -Dicafeoylspermidine	X	X	X	X						X	
7	6.53	322	325	264 (7), 179 (52), 161 (100)	Feruloyl-arabinoside						X					X
11	7.02	315	355	193 (100), 133 (47)	Feruloyl-glucoside		X									
14	7.64	315	309	145 (100), 119 (22), 117 (17)	Feruloyl-deoxyarabinoside						X	X	X			X
15	7.73	311	309	145 (100), 117 (51)	Feruloyl-deoxyarabinoside						X	X	X			X
17	8.03	326	339	324 (96), 175 (100), 160 (62)	Feruloyl-rhamnoside							X				X
18	8.10	326	339	177 (13), 175 (100), 134 (18)	Feruloyl-rhamnoside						X	X	X	X	X	X
20	8.25	326	339	177 (8), 175 (100), 160 (20)	Feruloyl-rhamnoside						X	X	X	X	X	X
22	8.31	322	193	161 (41), 134 (100), 133 (36)	Ferulic Acid	X	X	X	X	X						
29	9.90	320	415	304 (39), 253 (100), 135 (82)	Dicafeoylglycerol		X		X			X			X	
30	9.91	322	415	253 (54), 179 (91), 161 (100)	Dicafeoylglycerol		X		X		X	X			X	
31	10.00	326	415	179 (35), 161 (48), 135(100)	Dicafeoylglycerol				X		X				X	
37	10.46	315	399	163 (100), 161 (27), 119 (46)	p-coumaroyl-caffeoyl-glycerol		X		X							

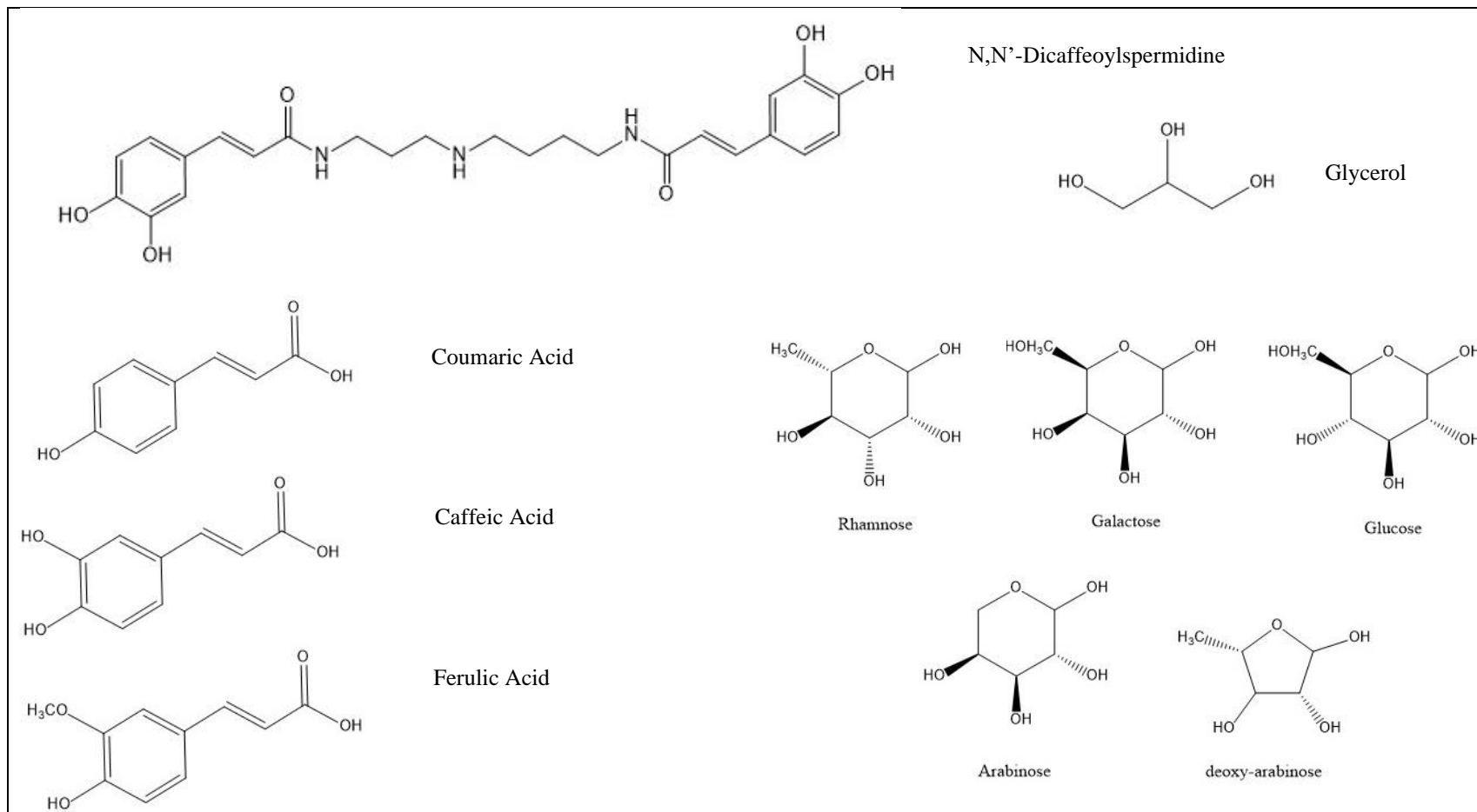


**Figure 10. Structures of the phenolic acid derivatives identified in sorghum phenotypes.**

### Identification of Flavanone Peaks

Peak 6 ( $t_R$  6.13 min,  $\lambda_{max} = 283$ ) had  $[M-H]^-$  at 449 m/z. Peak fragments had m/z at 135 ( $[M-H]^- - 314$ ), 287 ( $[M-H]^- - 162$ ), and 151 ( $[M-H]^- - 298$ ) (**Table 4**). The loss 162 resulting in the 287 m/z fragment represents the loss of an O-linked glycoside, resulting in the eriodictyol aglycone. The remaining fragments match known fragmentation patterns of eriodictyol-glycosides in literature (Gujer et al., 1986; Yang et al., 2012). Peak 6 was identified in the control sample of the Y/P phenotype (**Table 4**).

Peak 10 ( $t_R$  6.98 min,  $\lambda_{max} = 294$ ) had  $[M-H]^-$  at 433 m/z. Peak fragments had m/z at 271 ( $[M-H]^- - 162$ ), 177 ( $[M-H]^- - 256$ ), and 91 ( $[M-H]^- - 342$ ) (**Table 4**). Fragments were consistent with naringenin aglycone and the fragmentation pattern of naringenin. The loss of a glycoside (162) is evident as well. Therefore Peak 10 was identified as a naringenin-glycoside. It was found in the control and MAE treatment of the Y/P phenotype (**Table 4**).

Peak 25 ( $t_R$  9.68 min,  $\lambda_{max} = 287$ ) had  $[M-H]^-$  at 287 m/z. Peak fragments had m/z at 151 ( $[M-H]^- - 136$ ), 135 ( $[M-H]^- - 152$ ), and 107 ( $[M-H]^- - 180$ ) (**Table 4**). The fragmentation pattern, spectra profile, and parent mass all matched to known standards of eriodictyol. Peak 25 was therefore identified as eriodictyol. It was identified in the control and MAE treatments of the R/T and Y/P phenotypes (**Table 4**).

Peak 38 ( $t_R$  10.55 min,  $\lambda_{max} = 287$ ) had  $[M-H]^-$  at 271 m/z. Peak fragments had m/z at 151 ( $[M-H]^- - 120$ ), 119 ( $[M-H]^- - 152$ ), and 107 ( $[M-H]^- - 164$ ) (**Table 4**). The fragmentation pattern, spectra profile, and parent mass all matched to known standards



of naringenin. Peak 38 was therefore identified as naringenin. It was identified in both the control and MAE treatment of the R/T, R/P, and Y/P phenotypes (**Table 4**).

**Table 4** contains the identities of the flavanone compounds detected in each sorghum phenotype and the corresponding treatment. **Figure 11** displays the structures of these compounds.

**Table 4. Proposed identities of flavanone compounds found in sorghum phenotypes.**

Peak no.	Retention Time	$\lambda_{\max}$	[M-H] <sup>-</sup>	MS/MS Fragments	Proposed Identification	Sorghum Phenotype Detected									
						CTL W/T	CTL W/P	CTL R/T	CTL R/P	CTL Y/P	MAE W/T	MAE W/P	MAE R/T	MAE R/P	MAE Y/P
6	6.13	283	449	135 (100), 287 (75), 151 (81)	Eriodictyol-glycoside					X					
10	6.98	294	433	271 (100), 177 (73), 91 (93)	Naringenin-glycoside					X					X
25	9.68	287	287	151 (100), 135 (58), 107 (35)	Eriodictyol			X		X			X		X
38	10.55	287	271	151 (100), 119 (29), 107 (18)	Naringenin			X	X	X			X	X	X

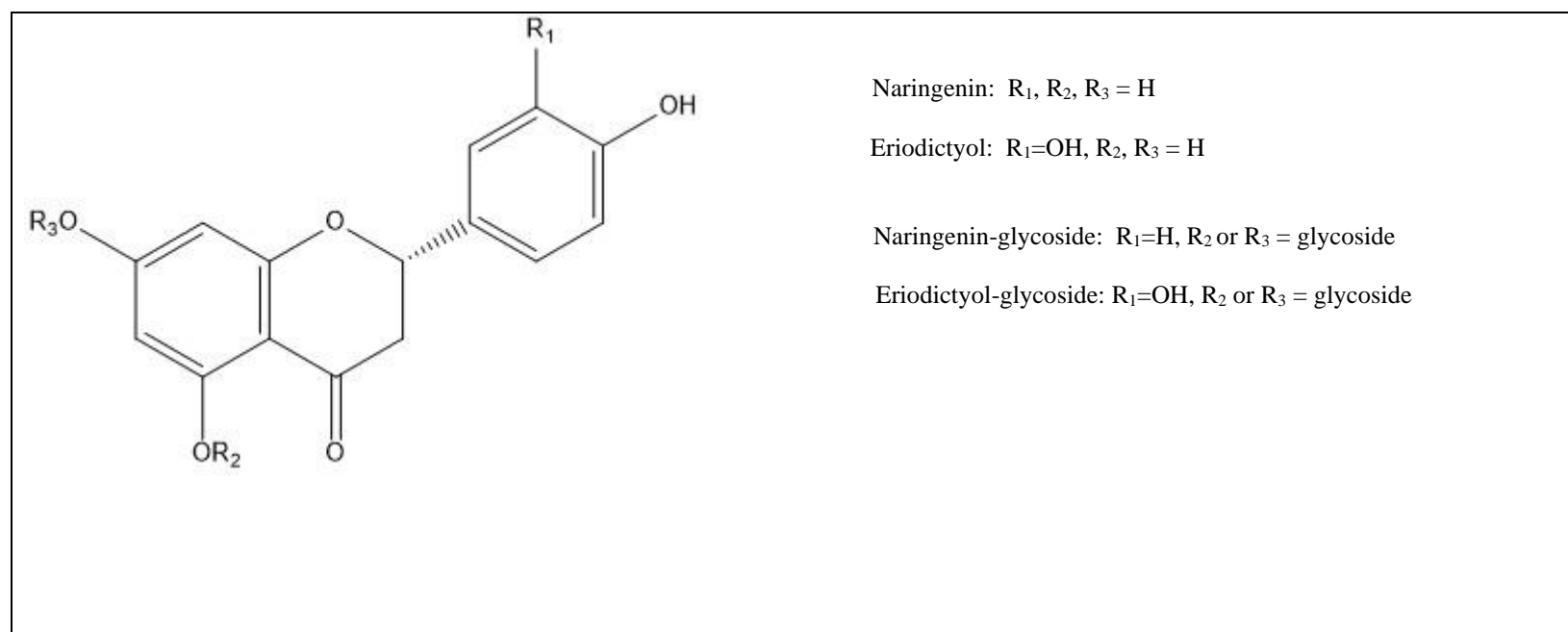


**Figure 11. Structures of proposed flavanone derivatives identified in sorghum phenotypes.**

### Identification of Flavone Peaks

Peak 32 ( $t_R$  10.07 min,  $\lambda_{max} = 344$ ) had  $[M-H]^-$  at 285 m/z. Peak fragments had m/z at 133 ( $[M-H]^- - 152$ ), 107 ( $[M-H]^- - 178$ ), and 65 ( $[M-H]^- - 220$ ) (**Table 5**). The fragmentation pattern, spectra profile, and parent mass all matched to known standards of luteolin. Peak 32 was identified in the control and MAE treatments of the W/T, R/T, and Y/P phenotypes (**Table 5**).

Peak 40 ( $t_R$  10.77 min,  $\lambda_{max} = 337$ ) had  $[M-H]^-$  at 269 m/z. Peak fragments had m/z at 151 ( $[M-H]^- - 118$ ), 117 ( $[M-H]^- - 152$ ), and 107 ( $[M-H]^- - 162$ ) (**Table 5**). The fragmentation pattern, spectra profile, and parent mass all matched to known standards of apigenin. Peak 40 was identified in control treatments of the W/T, W/P, and R/T phenotypes. It was also identified in the MAE treatment of the W/T and R/T phenotypes (**Table 5**).

**Table 5** contains the identities of the flavones detected in each sorghum phenotype and the corresponding treatment. **Figure 12** displays the structures of these compounds.

**Table 5. Proposed identities of flavone compounds found in sorghum phenotypes.**

Peak no.	Retention Time	$\lambda_{\max}$	[M-H] <sup>-</sup>	MS/MS Fragments	Proposed Identification	Sorghum Phenotype Detected									
						CTL W/T	CTL W/P	CTL R/T	CTL R/P	CTL Y/P	MAE W/T	MAE W/P	MAE R/T	MAE R/P	MAE Y/P
32	10.07	347	285	133 (96), 107 (65), 65 (100)	Luteolin	X		X		X	X		X		X
40	10.77	337	269	151 (69), 117 (100), 107 (93)	Apigenin	X	X	X			X		X		

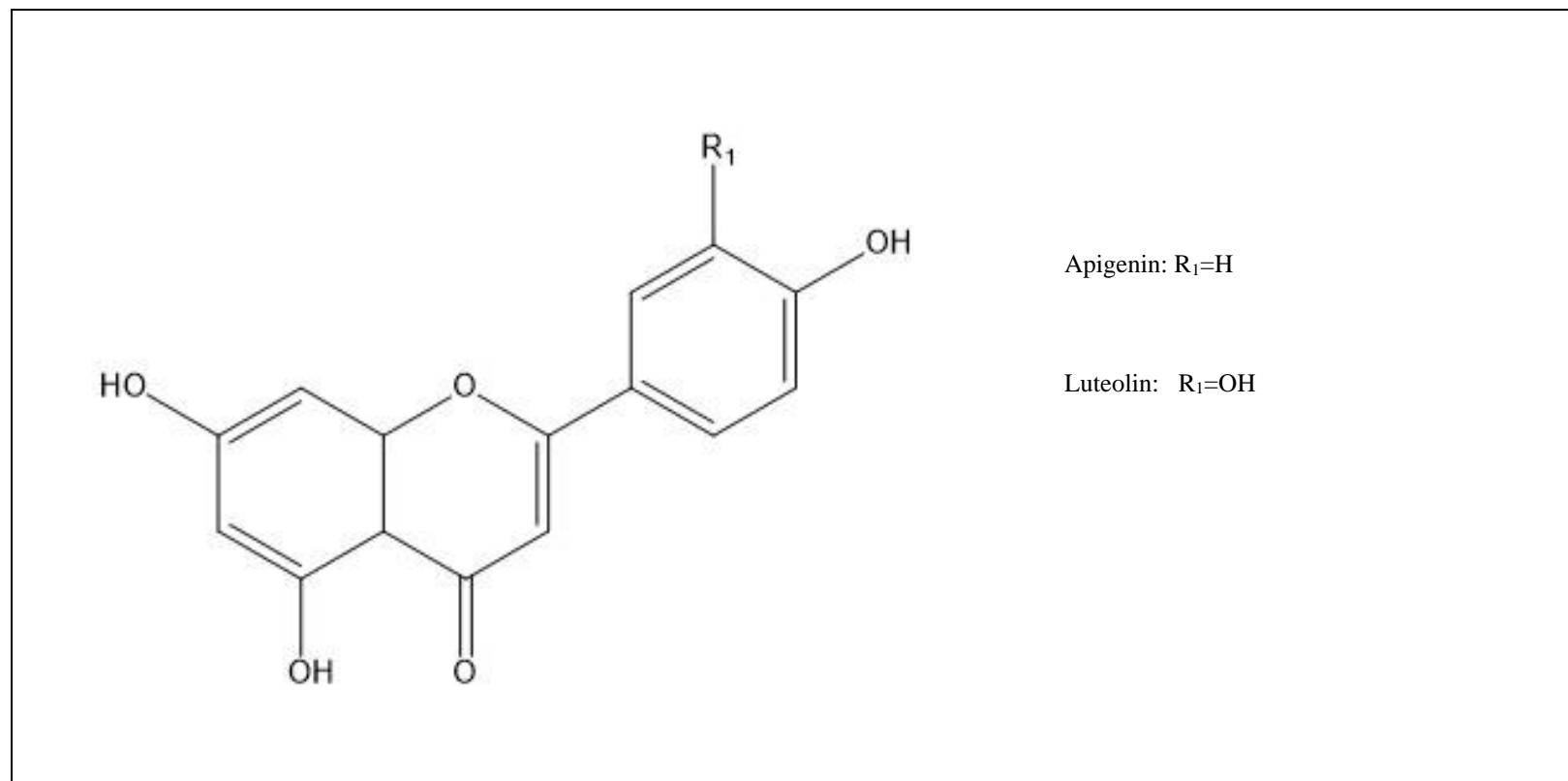


**Figure 12. Structures of proposed flavone derivatives identified in sorghum phenotypes**

### Identification of Anthocyanin Peaks

Peak 3 ( $t_R$  5.52 min,  $\lambda_{max} = 470$ ) had  $[M-H]^+$  at 417 m/z. The only peak fragment had m/z at 255 ( $[M-H]^- - 162$ ) (**Table 6**). The fragment at 255 is not only the result of a loss of a glycoside, but also the mass of an apigeninidin aglycone. Therefore, peak 3 was identified as an apigeninidin-glycoside and was detected in the control R/P phenotype (**Table 6**).

Peak 8 ( $t_R$  6.60 min,  $\lambda_{max} = 488$ ) had  $[M-H]^+$  at 271 m/z. Peak fragments had m/z at 179 ( $[M-H]^- - 92$ ), 173 ( $[M-H]^- - 98$ ), and 131 ( $[M-H]^- - 140$ ) (**Table 6**). The parent mass and fragment pattern, and spectra data are all consistent with known standards of luteolinidin. Luteolinidin was detected in the control extraction for the R/P and Y/P phenotypes, as well as the R/T, R/P, and Y/P phenotypes extracted through MAE (**Table 6**).

Peak 9 ( $t_R$  6.70 min,  $\lambda_{max} = 521$ ) had  $[M-H]^+$  at 287 m/z. Peak fragments had m/z at 185 ( $[M-H]^- - 102$ ), 167 ( $[M-H]^- - 120$ ), and 107 ( $[M-H]^- - 180$ ) (**Table 6**). The parent mass, fragment pattern, and spectra data are all consistent with cyanidin. Therefore peak 9 was identified as cyanidin and detected in the MAE treated R/T phenotype (**Table 6**).

Peak 12 ( $t_R$  7.28 min,  $\lambda_{max} = 473$ ) had  $[M-H]^+$  at 255 m/z. Peak fragments had m/z at 213 ( $[M-H]^- - 42$ ), 171 ( $[M-H]^- - 84$ ), and 69 ( $[M-H]^- - 186$ ) (**Table 6**). The parent mass, fragment pattern, and spectra data are all consistent with the standard for apigeninidin. Therefore peak 12 was identified as apigeninidin. Peak 12 was present in the control samples for W/P, R/P, Y/P phenotypes, and the MAE samples for W/P, R/T, R/P, and Y/P phenotypes (**Table 6**).

Peak 13 ( $t_R$  7.42 min,  $\lambda_{max} = 484$ ) had  $[M-H]^+$  at 285 m/z. Peak fragments had m/z at 271 ( $[M-H]^- - 14$ ), 242 ( $[M-H]^- - 43$ ), and 160 ( $[M-H]^- - 125$ ) (**Table 6**). The fragment peak at 271 is the aglycone of luteolinidin, and with a resulting loss of 14 consistent with OMe-Luteolinidin. Peak 13 was identified as OMe-Luteolinidin and was detected in R/P and Y/P phenotype control samples (**Table 6**).

Peak 16 ( $t_R$  7.74 min,  $\lambda_{max} = 481$ ) had  $[M-H]^+$  at 836 m/z. Peak fragments had m/z at 673 ( $[M-H]^- - 163$ ), 511 ( $[M-H]^- - 325$ ), and 385 ( $[M-H]^- - 451$ ) (**Table 6**). Spectral profile is consistent with other color compounds. However Peak 16 was unable to be identified at this time. Peak 16 was present in the control and MAE samples for the R/P phenotype (**Table 6**).

Peaks 19, and 21 ( $t_R$  8.13, and 8.30 min,  $\lambda_{max} = 470$ , and 477) had  $[M-H]^+$  at 269 m/z. Peak fragments had m/z at 254 ( $[M-H]^- - 15$ ), 226 ( $[M-H]^- - 43$ ), 197 ( $[M-H]^- - 72$ ), 169 ( $[M-H]^- - 100$ ), and 144 ( $[M-H]^- - 125$ ) (**Table 6**). Peak fragmentation for both 19 and 21 were consistent with methoxyapigeninidin standards. Standards of 5-OMe-apigeninidin and 7-OMe-apigeninidin were run to determine order of elution. The 7-OMe isomer was found to elute before the 5-OMe isomer on a reverse phase column. Therefore, peak 19 was identified as 7-OMe-apigeninidin and peak 21 was identified as 5-OMe-apigeninidin. Peak 19 was detected in both control and MAE samples of the W/P, R/P, and Y/P phenotypes, and the MAE sample of the R/T phenotype (**Table 6**). Peak 21 was identified in the control sample of the R/P phenotype (**Table 6**).

Peak 23 ( $t_R$  8.52 min,  $\lambda_{max} = 483$ ) had  $[M-H]^+$  at 283 m/z. Peak fragments had m/z at 269 ( $[M-H]^- - 14$ ), 226 ( $[M-H]^- - 57$ ), and 169 ( $[M-H]^- - 114$ ) (**Table 6**). The

fragment at 269 represents a loss of a methyl group resulting in a methoxyapigenidin. The remaining fragments are consistent with the breakdown the methoxyapigenidin standard. Therefore, Peak 21 was identified as 5,7-dimethoxyapigeninidin. Peak 23 was detected in the control and MAE samples for the R/P phenotype (**Table 6**).

Peak 34 ( $t_R$  10.19 min,  $\lambda_{max} = 322$ ) had  $[M-H]^-$  at 301 m/z. Peak fragments had m/z at 287 ( $[M-H]^- - 14$ ), 164 ( $[M-H]^- - 137$ ), and 125 ( $[M-H]^- - 176$ ) (**Table 6**). The spectral data and fragment mass at 287 (loss of methoxyl group) indicate that peak 34 is 7O-methoxycyanidin. This peak was present in the R/T phenotype after MAE (**Table 6**).

Peak 39 ( $t_R$  10.66 min,  $\lambda_{max} = 477$ ) had  $[M-H]^-$  at 655 m/z. Peak fragments had m/z at 271 ( $[M-H]^- - 206$ ), 165 ( $[M-H]^- - 312$ ), and 29 ( $[M-H]^- - 626$ ). These fragments are indicative of a luteolinidin derivative- with the fragment of 271 being a luteolinidin aglycone (**Table 6**). At this time this compound could not be completely identified. It was detected in the MAE sample of the R/P phenotype.

**Table 6** contains the identities of the anthocyanins detected in each sorghum phenotype and the corresponding treatment. **Figure 13** displays the structures of these compounds.

**Table 6. Proposed identities of anthocyanin compounds found in sorghum phenotypes.**

Peak no.	Retention Time	$\lambda_{\max}$	[M-H] <sup>+</sup>	MS/MS Fragments	Proposed Identification	Sorghum Phenotype Detected										
						CTL W/T	CTL W/P	CTL R/T	CTL R/P	CTL Y/P	MAE W/T	MAE W/P	MAE R/T	MAE R/P	MAE Y/P	
3	5.52	470	417	255 (100)	Apigeninidin-glycoside				X							
8	6.60	488	271	179 (87), 173 (100), 131 (61)	Luteolinidin				X	X			X	X	X	
9	6.70	521	287	185 (100), 167 (45), 107 (40)	Cyanidin								X			
12	7.28	473	255	213 (39), 171 (100), 69 (87)	Apigeninidin		X		X	X		X	X	X	X	
13	7.42	484	285	271 (30), 242 (100), 160 (32)	7-Ome-Luteolinidin				X	X						
16	7.74	481	836	673 (27) 511 (100) 385 (66)	Unknown Pigment:				X						X	
19	8.13	470	269	226 (100), 197 (21), 144 (27)	7-Ome-Apigeninidin		X		X	X		X	X	X	X	
21	8.30	477	269	254 (10) 226 (100) 169 (30)	5-Ome-Apigeninidin				X							
23	8.52	485	283	269 (100), 226 (85), 169 (26)	5,7 - Dimethoxyapigeninidin				X						X	
34	10.19	322	301	287(56) 164 (100), 125 (75)	7O-Methoxycyanidin								X			
39	10.66	477	655	271 (100), 165 (44), 29 (4)	Luteolinidin derivative										X	

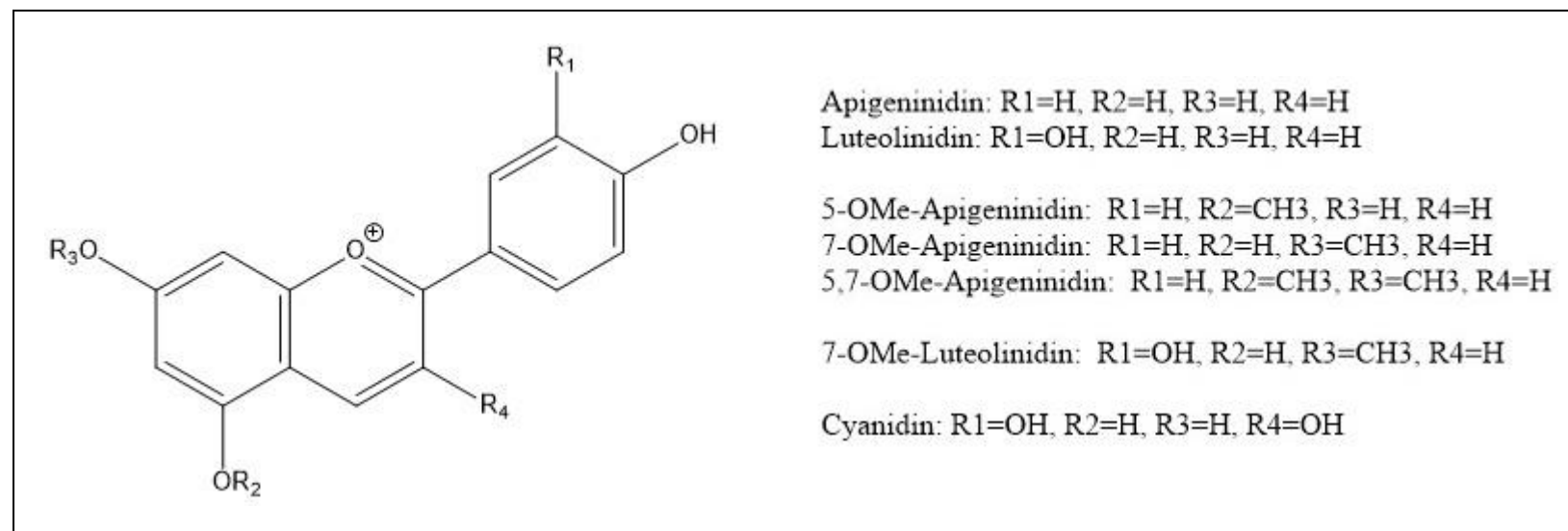


**Figure 13. Structures of proposed anthocyanidin derivatives identified in sorghum phenotypes**



### Effect of MAE on Phenolic Profile

Peaks were identified from the control and 600W 7 min MAE treatments for each sample. 41 compounds were profiled, 33 of which were structurally identified. These compounds and their proposed identities are located in **Table 2**. All sorghum phenotypes showed a change of phenolic profile upon MAE treatment compared to their control.

The phenolic acid profile of all phenotypes changed drastically upon microwave treatment. Some compounds, such as dicaffeoylglycerol (**Table 3**), remained present after microwave extraction. Other compounds detected in all sorghum phenotypes, such as ferulic acid, were undetectable following microwave extraction (**Table 3**). MAE saw the emergence of peaks not previously detected in the control extraction. Ferulic acid derivatives such as feruloyl-deoxyarabinoside and feruloyl-rhamnoside isomers are examples of these new compounds (**Table 3**). These new peaks are likely the result of the release of previously unextractable compounds bound to the cell wall material.

Monomeric flavonoids - flavones, flavanones, and 3-deoxyanthocyanins - were fairly unaffected by microwave treatment (**Tables 4, 5 and 6**). Flavones were detected primarily in sorghum phenotypes with white pericarp and tan secondary plant color, while flavanones were detected in pigmented phenotypes (**Table 4, 5**). 3-Deoxyanthocyanins were present in phenotypes with either pigmented pericarp, or purple secondary plant color (**Table 6**). The lack of significant change between control and MAE of the monomeric flavonoids indicates that they are stable to microwave energy.

## Quantification of Major Phenolic Peaks

Quantification data has been reported on dry basis, as a result of three separate runs. Only structurally identified compounds were quantified.

Overall, there was no statistical significance between phenolics quantified over all control and MAE samples. Significant differences between phenolic classes were present between the control and MAE samples. Overall, MAE treatment increased the amount of phenolic acids and their derivatives by 60 percent. The quantity of flavanones and flavones present decreased significantly, with MAE samples containing approximately half of the content of flavanones and about a third less flavones than was quantified in the control samples. Total anthocyanidin content did not change significantly between the treatment groups. The breakdown of the total phenolic content by compound type and treatment is displayed in **Table 7**.

While total phenolic content remained relatively similar between the control and MAE treatments, the changes that occurred between phenotypes due to MAE treatment was very different. **Table 8** displays these changes. The W/T, W/P, and R/T phenotypes showed a 5.4, 1.5, and 2.2 times greater total phenolic content after MAE treatment compared to the control. However, the total phenolic content quantified in the R/P and Y/P phenotypes decreased significantly by approximately half after MAE compared to the control. The following sections will discuss the changes amongst phenotypes in regard to phenolic acids, flavanones, flavones, and anthocyanidins.

**Table 7. Quantified phenolic content by compound type and treatment.**

Compound Type	Control Treatment	MAE Treatment
<i>Phenolic Acids</i>	163.0 ± 2.3 <sup>a</sup>	266.8 ± 1.0 <sup>b</sup>
<i>Flavanones</i>	176.1 ± 1.2 <sup>b</sup>	90.9 ± 2.4 <sup>a</sup>
<i>Flavones</i>	28.3 ± 0.8 <sup>b</sup>	18.1 ± 0.4 <sup>a</sup>
<i>Anthocyanidins</i>	50.5 ± 0.1 <sup>a</sup>	44.8 ± 0.5 <sup>a</sup>

Average µg/g sample dry basis (db) ± SD. Only structurally identified compounds were quantified.

<sup>a-b</sup> indicates statistical significance of phenolic compound between treatments (n=3, p<0.05).

**Table 8. Quantified phenolic content between treatments.**

Variety (phenotype)	Control Treatment	MAE Treatment
<i>ATx635/RTx436</i> (W/T)	18.6±0.6 <sup>a</sup>	98.1±0.7 <sup>b</sup>
<i>17CS5417</i> (W/P)	57.3±3.5 <sup>a</sup>	84.4±1.0 <sup>b</sup>
<i>NK8830</i> (R/T)	36.6±0.4 <sup>a</sup>	81.7±1.6 <sup>b</sup>
<i>ATx2911</i> (R/P)	157.8±2.2 <sup>b</sup>	71.4±1.0 <sup>a</sup>
<i>ATX642/RO6321</i> (Y/P)	147.6±1.5 <sup>b</sup>	85.0±1.4 <sup>a</sup>

Average µg/g sample dry basis (db) ± SD. Only structurally identified compounds were quantified.

<sup>a-b</sup> indicates statistical significance of phenolic compound between treatments (n=3, p<0.05).

#### *Quantification of Phenolic Acids*

Phenolic acid content in the MAE treated samples was generally 60% higher than the control (**Table 9**). The greatest increase was seen in the W/T phenotype with an 11 times greater quantified phenolic acid content in the MAE samples compared to the control (**Table 9**). In contrast to the other phenotypes, the R/P phenotype saw a reduction in quantified phenolic acid content (**Table 9**). In this case, the MAE treatment yielded a third of the content of the control sample. The other phenotypes, W/P, R/T, and Y/P, yielded 1.6, 5, and 7 times the quantified phenolic acid content in MAE as

compared to the control (**Table 9**). The increases were largely attributed to the release of cell wall bound phenolics. Because the R/P phenotype has the greatest content of extractable ferulic acid in the control, the decrease in ferulic acid following MAE suggests that rapidly extractable free phenolic acids are easily degraded under MAE. Conversely, the slow release of bound phenolics may have a protective effect against their degradation due to MAE. This is furthermore supported when observing the specific compounds that are present in control samples, versus the compounds detected in the MAE samples of the same phenotypes (**Table 9**). The content of ferulic acid is the greatest example of this. It is detected in all the control samples, and is completely undetected in any of the subsequent MAE samples (**Table 9**). Likewise, compounds such as the feruloyl-rhamnoside isomers detected and quantified in all MAE samples are not detectable in the control extractions (**Table 9**).

The great discrepancy between the control and MAE R/P phenotype compared to the other samples is likely due to the high amount of free phenolic acids compared to the other phenotypes. The quantity of degradation and loss of those compounds could not be compensated for by the release of the bound phenolics, leading to an overall loss in quantified phenolic acid content. The other phenotypes likely underwent the same degradations, but since their content of free phenolic acids was much lower than the R/P phenotype, the quantity of released bound phenolics quickly overcame that loss. This is supported in part by the W/P phenotype which had the second lowest increase in phenolic acid content (1.6 times increase), but second highest starting content of the phenotypes selected for this study (48.5 ug/g) (**Table 9**). The large loss of phenolic

content seen in **Table 8** is likely due to this degradation caused by MAE in the phenotypes, such as R/P and Y/P, which contained higher amounts of easily extractable phenolics than the other phenotypes tested.

**Table 9. Quantification of detected phenolic acid derivatives in each phenotype.**

Proposed ID	Concentration ( $\mu\text{g/g}$ sample, dry basis) of phenolics by phenotype									
	CTL W/T	CTL W/P	CTL R/T	CTL R/P	CTL Y/P	MAE W/T	MAE W/P	MAE R/T	MAE R/P	MAE Y/P
2-O-Caffeoylglycerol										1.3 $\pm$ 0.5
1-O-Caffeoylglycerol		1.9 $\pm$ 0.1		4.9 $\pm$ 0.6						
Feruloylgalactoside						3.7 $\pm$ 0.7				3.5 $\pm$ 0.5
N, N' - Dicaffeoylspermidine	3.6 $\pm$ 0.2	4.0 $\pm$ 1.5	3.1 $\pm$ 0.6	11.1 $\pm$ 1.6					2.1 $\pm$ 0.2	
Feruloyl-arabinoside						4.4 $\pm$ 0.1				1.9 $\pm$ 0.5
Feruloyl-glucoside		5.0 $\pm$ 0.9								
Feruloyl- deoxyarabinoside						5.1 $\pm$ 0.4	3.8 $\pm$ 0.3	2.3 $\pm$ 0.4		2.0 $\pm$ 1.7
Feruloyl- deoxyarabinoside							3.6 $\pm$ 0.2	1.9 $\pm$ 1.4		0.9 $\pm$ 0.8
Feruloyl-rhamnoside							4.8 $\pm$ 0.9			1.4 $\pm$ 1.2
Feruloyl-rhamnoside						17.2 $\pm$ 0.3	13.2 $\pm$ 2.4	8.7 $\pm$ 0.3	5.5 $\pm$ 0.1	7.6 $\pm$ 1.9
Feruloyl-rhamnoside						37.8 $\pm$ 0.8	38.5 $\pm$ 1.7	18.7 $\pm$ 0.2	6.4 $\pm$ 0.4	21.9 $\pm$ 1.0
Ferulic Acid	4.5 $\pm$ 0.6	13.7 $\pm$ 10.7	3.2 $\pm$ 0.2	11.4 $\pm$ 2.1	5.8 $\pm$ 0.2					
Dicaffeoylglycerol		17.0 $\pm$ 2.1		21.2 $\pm$ 4.4			9.2 $\pm$ 1.3		3.7 $\pm$ 0.7	
Dicaffeoylglycerol		3.8 $\pm$ 1.4		12.1 $\pm$ 0.1		13.7 $\pm$ 2.1	4.3 $\pm$ 0.4		3.3 $\pm$ 0.1	
Dicaffeoylglycerol				28.9 $\pm$ 4.9		7.0 $\pm$ 0.3			5.7 $\pm$ 1.2	
p-coumaroyl-caffeoyl- glycerol		3.0 $\pm$ 0.3		4.7 $\pm$ 0.2						
<b>Total Phenolic Acids</b>	<b>8.1<math>\pm</math>0.4</b>	<b>48.5<math>\pm</math>4.2</b>	<b>6.3<math>\pm</math>0.5</b>	<b>94.3<math>\pm</math>2.7</b>	<b>5.8<math>\pm</math>0.2</b>	<b>90.6<math>\pm</math>0.9</b>	<b>77.5<math>\pm</math>1.3</b>	<b>31.6<math>\pm</math>0.7</b>	<b>26.7<math>\pm</math>0.6</b>	<b>40.5<math>\pm</math>1.2</b>

Average  $\mu\text{g/g}$  sample dry basis  $\pm$  SD. Only structurally identified compounds were quantified. Blank or ND= Not Detected.

### *Quantification of Flavanones*

Flavanone content decreased overall between the control and MAE samples (**Table 7**). Flavanones were undetected in the white pericarp phenotypes, and content did not change significantly between the control and MAE treatments in the red phenotypes (**Table 10**). A large decrease was recorded in the Y/P phenotype, with the MAE sample

containing a third of the flavanones quantified than the control sample. This is the cause of the overall change in quantified flavanone content noted in **Table 7**. The loss in flavanone content in the Y/P phenotype comes from the degradation of naringenin and eriodictyol, as well as eriodictyol-glycoside (**Table 10**). Overall, aglycone forms of flavanones tended to be less susceptible to degradation and stable during MAE. Glycoside forms, especially eriodictyol-glycoside degraded during MAE treatment (**Table 10**). This loss of flavanones to MAE would also contribute to the overall loss of phenolic compounds seen in **Table 8**.

**Table 10. Quantification of detected flavanones in each phenotype.**

Proposed ID	Concentration ( $\mu\text{g/g}$ sample, dry basis) of phenolics by phenotype									
	CTL W/T	CTL W/P	CTL R/T	CTL R/P	CTL Y/P	MAE W/T	MAE W/P	MAE R/T	MAE R/P	MAE Y/P
Eriodictyol-glycoside					18.8 $\pm$ 1.8					
Naringenin-glycoside					4.3 $\pm$ 3.2					3.8 $\pm$ 0.4
Eriodictyol			14.0 $\pm$ 0.3		82.0 $\pm$ 1.0			14.6 $\pm$ 4.1		28.8 $\pm$ 2.6
Naringenin			7.7 $\pm$ 0.7	28.9 $\pm$ 1.7	20.5 $\pm$ 2.1			11.5 $\pm$ 3.4	24.5 $\pm$ 2.9	7.7 $\pm$ 3.1
<b>Total Flavanones</b>	<b>ND</b>	<b>ND</b>	<b>21.7<math>\pm</math>0.6</b>	<b>28.9<math>\pm</math>1.7</b>	<b>125.6<math>\pm</math>2.2</b>	<b>ND</b>	<b>ND</b>	<b>26.1<math>\pm</math>3.8</b>	<b>24.5<math>\pm</math>2.9</b>	<b>40.3<math>\pm</math>2.4</b>

Average  $\mu\text{g/g}$  sample dry basis  $\pm$  SD. Only structurally identified compounds were quantified.

Blank or ND= Not Detected.

### *Quantification of Flavones*

Flavones decreased overall between the MAE and control samples (**Table 7**). The only phenotype where flavone content appears to increase is the W/P phenotype, which effectively doubled. Flavones were not detected in the R/P phenotype in either the control or MAE sample (**Table 11**). All other phenotypes saw a decrease in flavone content between the control and MAE sample. The W/T phenotype retained about 70% of the flavone content after MAE, the R/T phenotype retained 55% after MAE, and the

Y/P phenotype retained 20% after MAE (**Table 11**). The low levels of the flavones quantified across phenotypes would have a limited impact on the overall phenolic content, and any significant losses or gains between treatments would play a negligible roll in the increases or decreases noted in **Table 8**.

**Table 11. Quantification of detected flavones in each phenotype.**

Proposed ID	Concentration ( $\mu\text{g/g}$ sample, dry basis) of phenolics by phenotype									
	CTL W/T	CTL W/P	CTL R/T	CTL R/P	CTL Y/P	MAE W/T	MAE W/P	MAE R/T	MAE R/P	MAE Y/P
Luteolin	2.8 $\pm$ 0.1		7.2 $\pm$ 0.2		7.2 $\pm$ 1.5	2.2 $\pm$ 0.1	1.4 $\pm$ 0.1	2.7 $\pm$ 0.4		1.5 $\pm$ 0.7
Apigenin	7.7 $\pm$ 1.1	2.0 $\pm$ 0.4	1.3 $\pm$ 0.2			5.2 $\pm$ 0.4	3.0 $\pm$ 0.1	2.1 $\pm$ 0.1		
<b>Total Flavones</b>	<b>10.5<math>\pm</math>0.8</b>	<b>2.0<math>\pm</math>0.4</b>	<b>8.6<math>\pm</math>0.2</b>	<b>ND</b>	<b>7.2<math>\pm</math>1.5</b>	<b>7.4<math>\pm</math>0.3</b>	<b>4.4<math>\pm</math>0.1</b>	<b>4.8<math>\pm</math>0.3</b>	<b>ND</b>	<b>1.5<math>\pm</math>0.7</b>

Average  $\mu\text{g/g}$  sample dry basis  $\pm$  SD. Only structurally identified compounds were quantified.

Blank or ND= Not Detected.

#### *Quantification of 3-Deoxyanthocyanins*

3-Deoxyanthocyanin content did not change significantly between control and MAE treatment overall (**Table 7**). The most unusual observation was seen in the R/T phenotype where there was no detectable 3-deoxyanthocyanins in the control group, but upon MAE treatment many were detected (**Table 12**). As 3-deoxyanthocyanins are not usually found in mature sorghum grain, the appearance of these compounds in the MAE R/T sample is likely due to the presence of tannins in this phenotype. Tannins have been shown to undergo oxidative depolymerization under MAE (Ravisankar et al., 2018). The presence of these compounds in the control and MAE samples of the other phenotypes is explained by their secondary plant color. Those with a tan secondary color (W/T) lacked a significant presence of the 3-deoxyanthocyanins, while those with

pigmented secondary color (W/P, R/P, Y/P) contained quantifiable levels before and after MAE treatment.

**Table 12. Quantification of detected anthocyanidins in each phenotype by treatment.**

Proposed ID	Concentration ( $\mu\text{g/g}$ sample, dry basis) of phenolics by phenotype									
	CTL W/T	CTL W/P	CTL R/T	CTL R/P	CTL Y/P	MAE W/T	MAE W/P	MAE R/T	MAE R/P	MAE Y/P
Apigeninidin-glycoside				4.4 $\pm$ 1.5						
Luteolinidin				2.5 $\pm$ 0.4	1.4 $\pm$ 0.2			1.6 $\pm$ 1.0	0.4 $\pm$ 0.2	0.4 $\pm$ 0.2
Cyanidin								2.7 $\pm$ 1.8		
Apigeninidin		5.0 $\pm$ 0.1		9.3 $\pm$ 2.9	4.7 $\pm$ 1.1		1.8 $\pm$ 0.1	3.5 $\pm$ 0.4	13.8 $\pm$ 0.8	1.5 $\pm$ 0.2
7-OMe-Luteolinidin				1.9 $\pm$ 2.1	0.5 $\pm$ 0.1	0.2 $\pm$ 0.1				
7-OMe-Apigeninidin		1.7 $\pm$ 0.0					0.7 $\pm$ 0.1	0.7 $\pm$ 0.1	1.3 $\pm$ 0.3	0.8 $\pm$ 0.1
5-OMe-Apigeninidin				1.8 $\pm$ 0.2						
5,7 - Dimethoxyapigeninidin				9.7 $\pm$ 1.5					1.2 $\pm$ 0.3	
Methoxycyanidin								10.8 $\pm$ 0.2		
Luteolinidin derivative									2.9 $\pm$ 1.4	
<b>Total Anthocyanidins</b>	<b>ND</b>	<b>6.8<math>\pm</math>0.1</b>	<b>ND</b>	<b>34.7<math>\pm</math>1.7</b>	<b>9.0<math>\pm</math>0.6</b>	<b>0.2<math>\pm</math>0.1</b>	<b>2.6<math>\pm</math>0.1</b>	<b>19.2<math>\pm</math>0.9</b>	<b>20.1<math>\pm</math>0.7</b>	<b>2.7<math>\pm</math>0.2</b>

Average  $\mu\text{g/g}$  sample dry basis  $\pm$  SD. Only structurally identified compounds were quantified.

Blank or ND= Not Detected.

## Conclusion

The type and structure of phenolics varied greatly between phenotypes. The control treatment contained more flavones and flavanones than MAE – likely due to the breakdown of these compounds during microwave treatment. MAE treatment not only generally contained higher amounts of phenolic acid derivatives compared to control, but also structurally different phenolic acids. The breakdown of free phenolic acids under MAE, and simultaneous release of bound phenolics, is responsible for this profile change. The abundance of the compounds released after MAE is attributed to the



destruction of cell wall polysaccharides causing the release of previously bound phenolic acid derivatives, such as the feruloyl-rhamnosides, seen across phenotypes.

## CHAPTER V

### EFFECT OF MICROWAVE ASSISTED EXTRACTION (MAE) ON EXTRACTABLE PHENOLICS AND ANTIOXIDENT CAPACITY OF SORGHUM BRANS

#### Sorghum Phenotypes Selected for Analysis

**Table 13. Sorghum phenotypes used in this study and notations**

Phenotype Code	Sorghum Variety	Pericarp Color	Secondary Plant Color	Sorghum Type
W/T	ATx635/RTx436	White	Tan	I
W/P	17CS5417	White	Purple	I
R/T	NK8830	Red	Tan	III
R/P	ATx2911	Red	Purple	I
Y/P	ATx436/RO6321	Lemon Yellow	Purple	I

#### Effect of MAE on Total Extractable Phenolic Content

Of the sorghum brans tested, the white pericarp samples showed the greatest increase in total phenolics between the control and MAE samples (**Table 8**). Both white sorghums, W/T and W/P, saw a significant increase in total phenolics after MAE treatment compared to the control (**Table 8**). On average, the MAE treatment the total extractable phenolics was 3.5 and 2.8 times greater for the W/T and W/P, respective, phenotypes compared to control (**Figure 14, 15**). The total phenolic content of the MAE treated R/T sorghum was 2.7 times greater than the total extractable phenolics for the control treatment (**Figure 16**). This greatly contrasts the other red phenotype (R/P),

which showed no significant difference between the control and MAE treated samples (**Figure 17**). The lemon yellow sorghum phenotype, Y/P, also showed no significant difference between MAE and control samples (**Figure 18**). This trend follows the one noted in the previous chapter where the W/T, W/P and R/T phenotypes all saw a quantified increase in quantifiable phenolic compounds, whereas the R/P and Y/P phenotypes saw a decrease in compounds quantified by UPLC following MAE (**Table 8**).

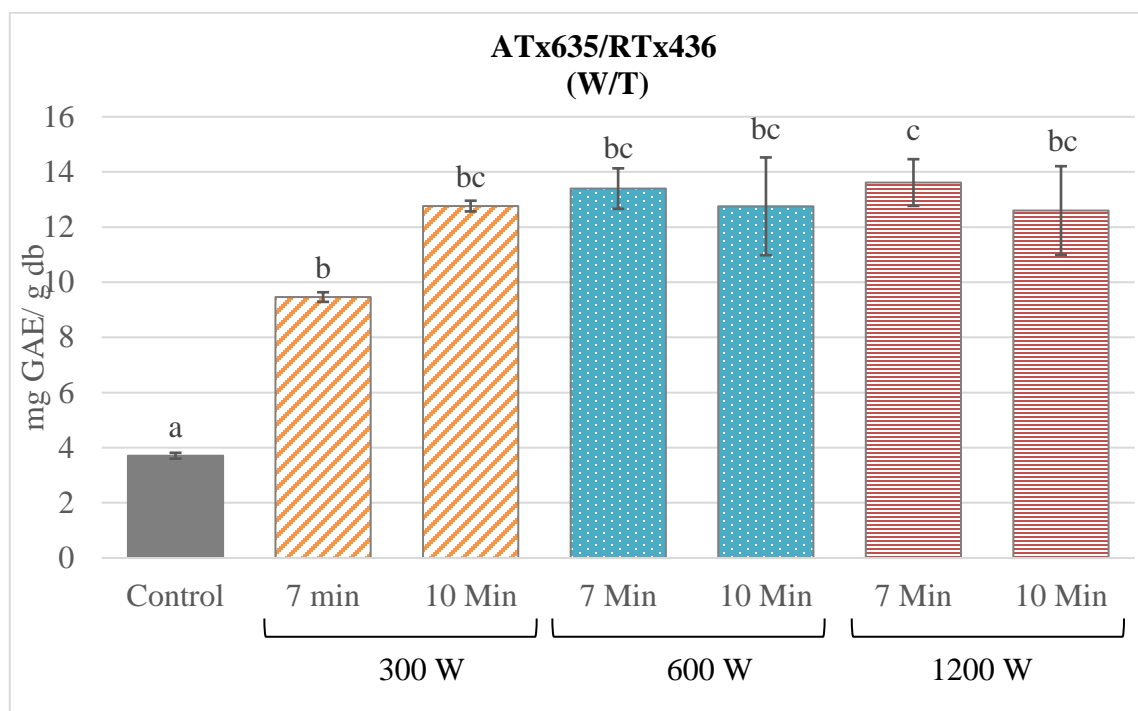


**Figure 14. Total extractable phenolics for control and MAE treated ATx635/RTx436 (W/T) sorghum bran. Error bars =  $\pm$  Standard Deviation (n=3) \*a-c: denotes statistical significance (p<0.05)**

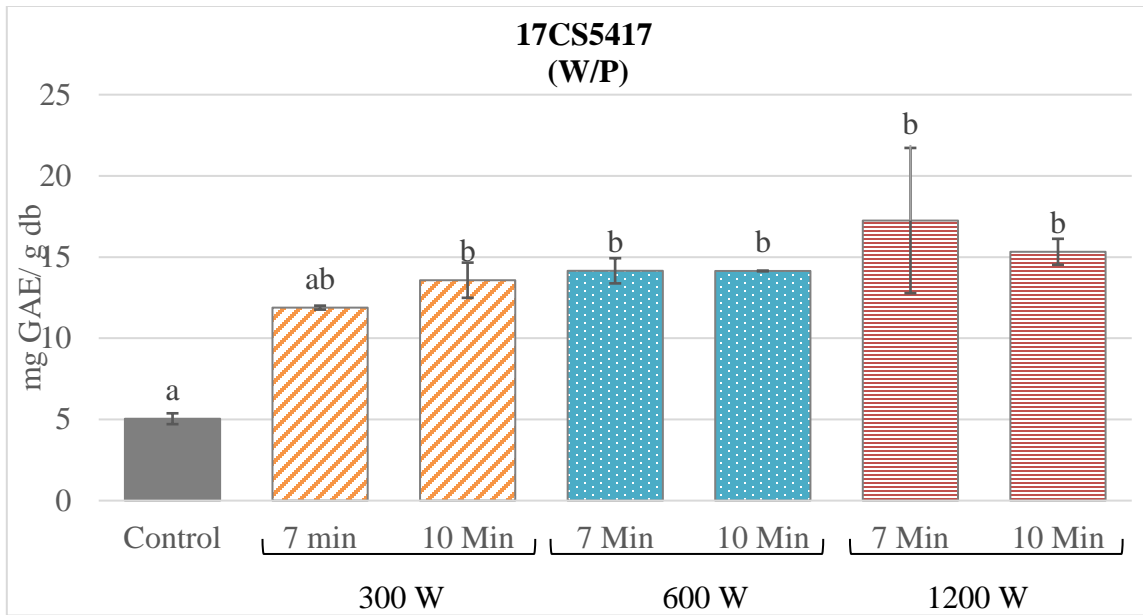


**Figure 15. Total extractable phenolics for control and MAE treated 17CS5417 (W/P) sorghum bran. Error bars =  $\pm$  Standard Deviation (n=3) \*a-b: denotes statistical significance ( $p < 0.05$ )**

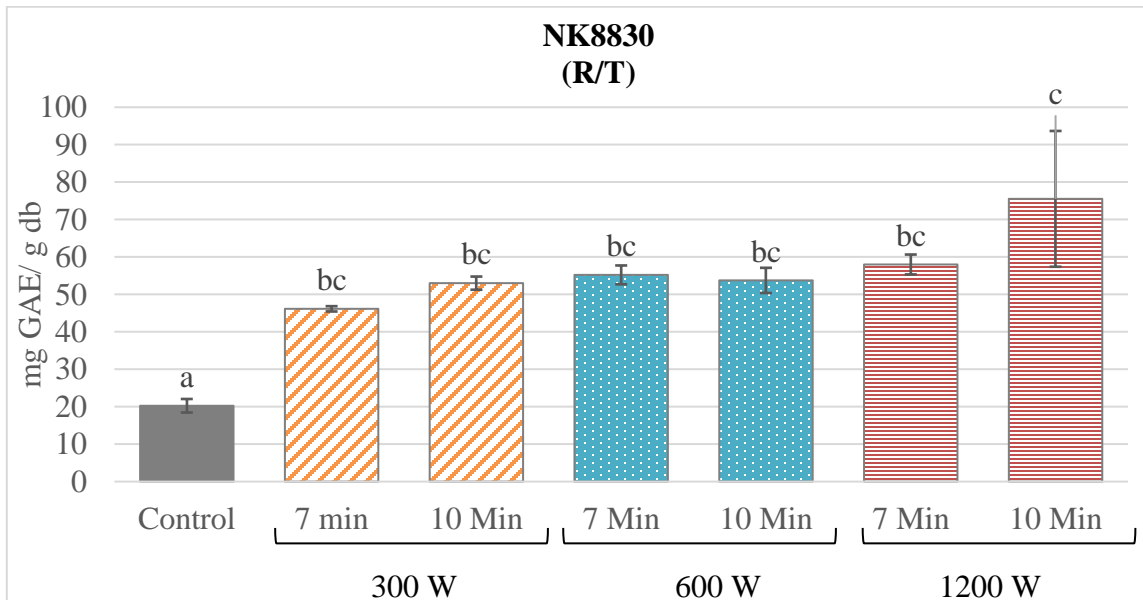


**Figure 16. Total extractable phenolics for control and MAE treated NK8830 (R/T) sorghum bran. Error bars =  $\pm$  Standard Deviation (n=3) \*a-c: denotes statistical significance ( $p < 0.05$ )**

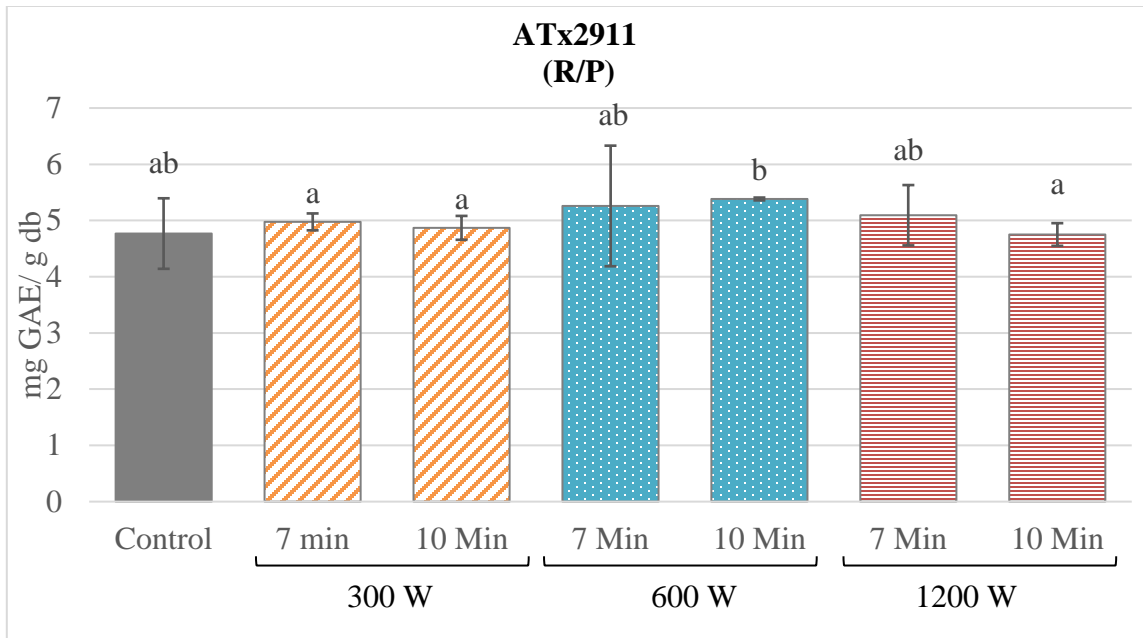


**Figure 17. Total extractable phenolics for control and MAE treated ATx2911 (R/P) sorghum bran. Error bars =  $\pm$  Standard Deviation (n=3) \*a-b: denotes statistical significance ( $p < 0.05$ )**

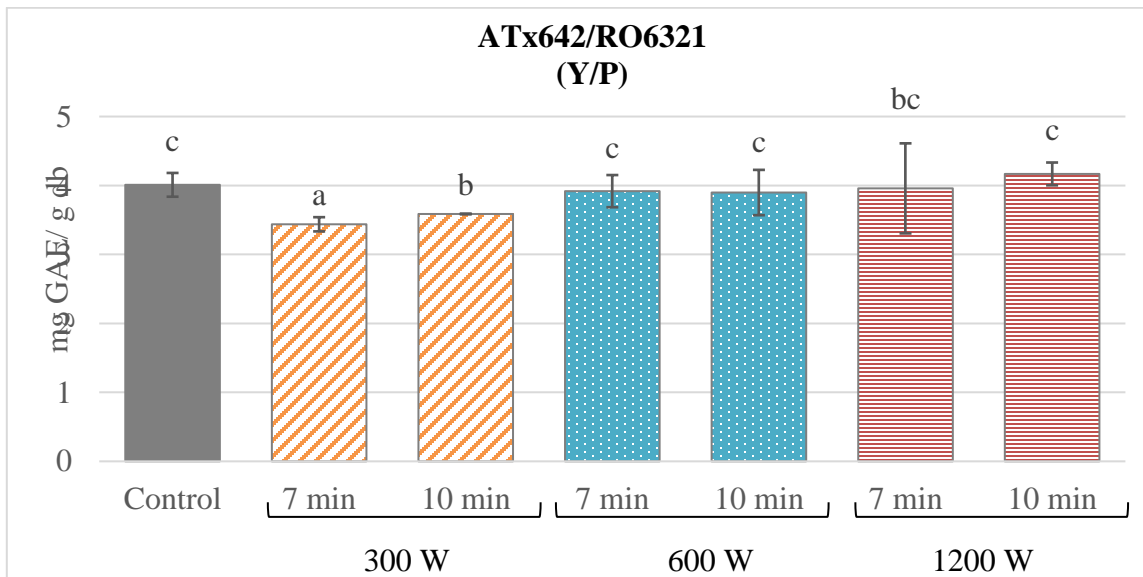


**Figure 18. Total extractable phenolics for control and MAE treated ATx642/RO6321 (Y/P) sorghum bran. Error bars =  $\pm$  Standard Deviation (n=3) \*a-c: denotes statistical significance ( $p < 0.05$ )**

The two non-pigmented pericarp sorghum phenotypes, W/T and W/P, both showed large increases in total extractable phenolics following MAE treatment. As discussed in chapter IV, these phenotypes contained many phenolic acid derivatives in MAE that were undetected in the control samples. The most prominent peaks were feruloyl-rhamnosides which emerged following MAE. These, as well as other minor feruloyl peaks, can also be identified in the MAE samples of the other sorghum phenotypes. These compounds are likely the result of the breakdown of cell wall material which is known to contain high amounts of ferulic acid (Dykes et al., 2011; Girard and Awika, 2018). This breakdown and subsequent release of smaller antioxidant compounds is likely the cause of the large increase in phenolic content, as measured by the Folin test in this chapter, seen in both white phenotypes.

Tannin presence in pigmented pericarp seemed to play a role in the increase of total extractable phenolics detected in the R/T sample. The red tannin sorghum, R/T, showed a significantly higher amount of total extractable phenolics compared to control. The R/P and Y/P phenotypes showed no difference in phenolic content between the MAE and control treatments. Peak identification in Chapter 4 exhibited new peaks associated with tannin sorghum. Methoxycyanidin, and cyanidin were only detected in the tannin sorghum. Upon breakdown of the condensed tannin polymers in sorghum bran, there would be a large increase in monomers and dimers present in the sample, and would explain the increase in phenolic content. Therefore, these compounds likely contributed to the large increase in total extractable phenolics in tannin sorghum,

whereas the other pigmented, type I phenotypes (R/P, Y/P) showed no significant increase in phenolic content following MAE.

Overall, MAE treatments were able to either match or increase the total extractable phenolics from the samples. The largest increases were seen in the non-pigmented (W/T and W/P) and tannin phenotypes (R/T), whereas the phenotypes which were non-tannin and pigmented (R/P and Y/P) showed no significant difference from the control treatment. The increase under MAE is partly attributed to the breakdown of condensed tannins into monomers in the tannin phenotype (R/T), and the breakdown of phenolic acid rich cell wall material in the white sorghum phenotypes (W/T and W/P) during microwave assisted extraction. In general, MAE matched or significantly increased the phenolic content of sorghum bran, making it a viable method to extract the compounds from sorghum.

### **Effect of MAE on Antioxidant Capacity**

The MAE treatment of the W/T phenotype resulted in a 3.4 times greater antioxidant capacity than the control method (**Figure 19**). The MAE treatment for the W/P phenotype was significantly greater than the control, and resulted in a 2.9 times greater antioxidant capacity on average (**Figure 20**). For both white phenotypes, the antioxidant capacity increased during the 2 minutes to 7 minutes treatments, then slightly decreased after 10 minutes of treatment. The exception to this is the 10 min treatment at 300W. Overall, both white, non-pigmented pericarp phenotypes exhibited large increases in total antioxidant capacity, similar to the total phenolic content data (**Figure**

**19, 20** and **Figures 14, 15**). This is likely attributed to the breakdown of the cell wall material producing large amounts of ferulic acid derivatives as discussed in chapter IV, and then further breakdown of antioxidant compounds into non-phenolic compounds under the longer, more powerful treatments.

Likewise, similar to the data reported from the Folin test in **Figure 16**, the R/T phenotype also showed a significant increase in antioxidant capacity under MAE, increasing on average by 2.6 times the amount seen in the control (**Figure 21**). Of the pigmented phenotypes, the R/T saw the largest increase in total antioxidant capacity. Since this is a Type III sorghum, the increase can likely be attributed to the breakdown of the condensed tannins into flavonoid monomers and dimers over the longer and more powerful treatments. The acidic environment likely also aided the extraction and breakdown of the condensed tannins. This release and breakdown would cause an increase of antioxidant capacity due to the greater abundance of phenolic compounds.

MAE treatment of the R/P phenotype produced an antioxidant capacity 1.2 times greater than the control (**Figure 22**). This relatively low increase in antioxidant capacity due to MAE mimics the change reflected in the total phenolic content data (**Figure 17**). In the Y/P phenotype, antioxidant capacity was 1.9 times greater after MAE than the control (**Figure 23**). Surprisingly, the Y/P sample exhibited an increase in antioxidant capacity due to MAE in contrast to the total phenolic content data (**Figure 18**). This



suggests some MAE degradation products that were not Folin reactive, are present in this phenotype.

Overall, the R/T phenotype had the highest antioxidant content between all phenotypes tested. The maximum antioxidant capacity achieved under MAE (862  $\mu\text{mol}$  Trolox equivalents/ g sample db) (**Figure 21**) was over 3 times greater than any other sample, the closest being from the R/P phenotype (263  $\mu\text{mol}$  Trolox equivalents/ g sample db) (**Figure 22**).

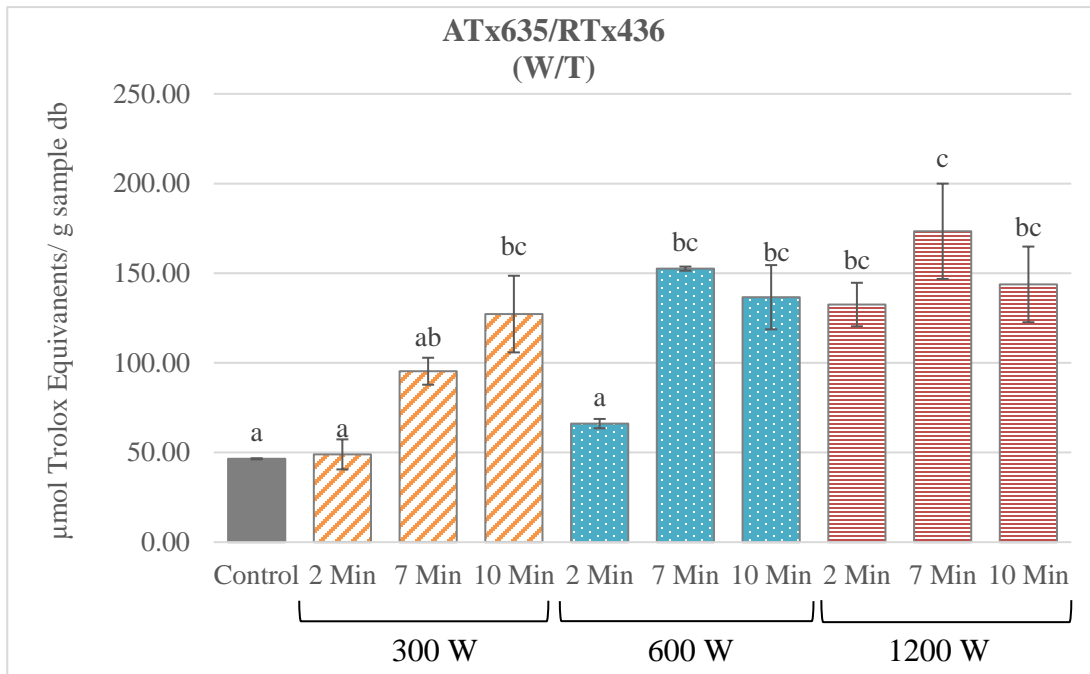


**Figure 19. Antioxidant capacity measured by trolox equivalents (TE) for control and MAE treated ATx 635/RTx436 sorghum bran. Error bars =  $\pm$  Standard Deviation (n=3) \*a-c: denotes statistical significance ( $p < 0.05$ )**

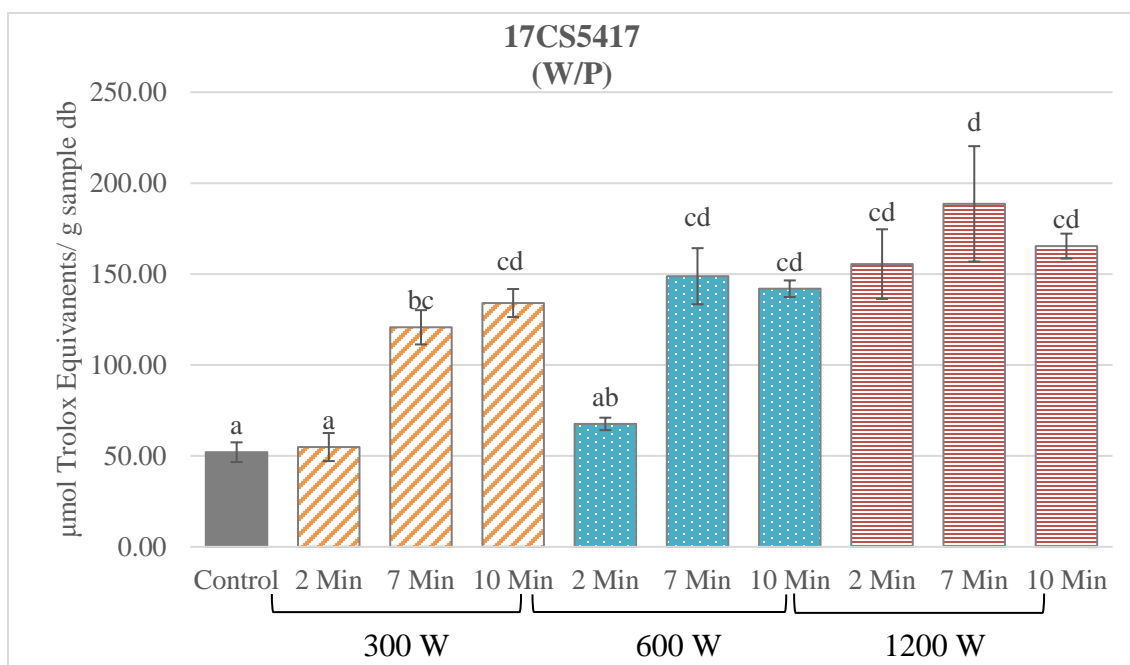


**Figure 20. Antioxidant capacity measured by trolox equivalents (TE) for control and MAE treated 17CS5417 sorghum bran. Error bars =  $\pm$  Standard Deviation (n=3) \*a-c: denotes statistical significance ( $p < 0.05$ )**

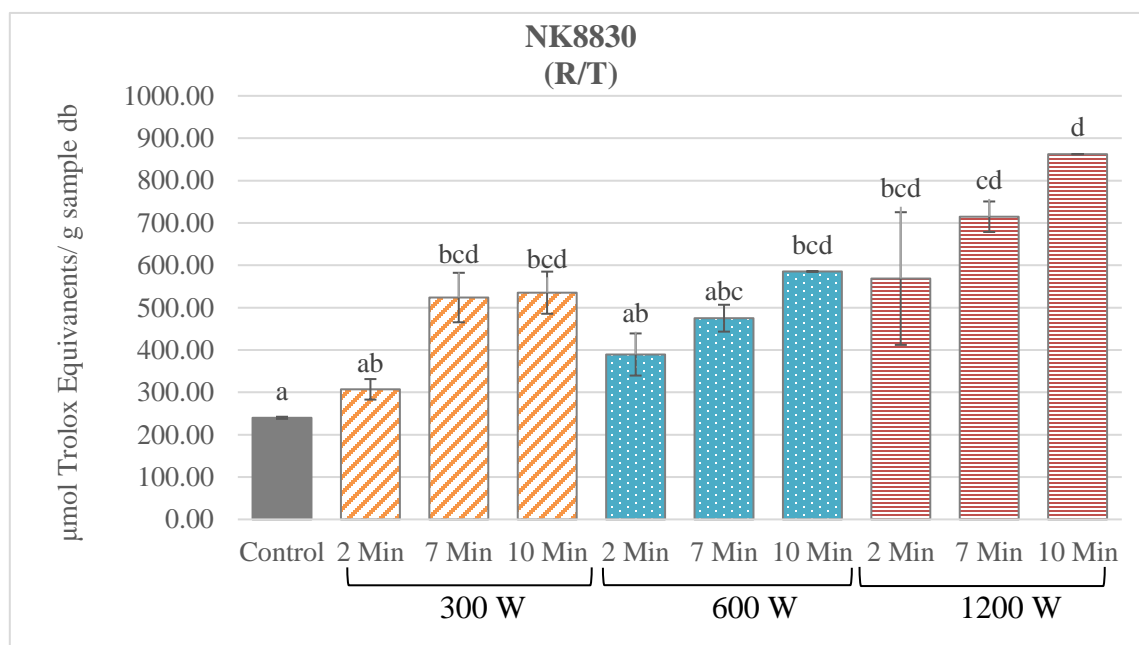


**Figure 21. Antioxidant capacity measured by trolox equivalents (TE) for control and MAE treated NK8830 sorghum bran. Error bars =  $\pm$  Standard Deviation (n=3) \*a-c: denotes statistical significance ( $p < 0.05$ )**

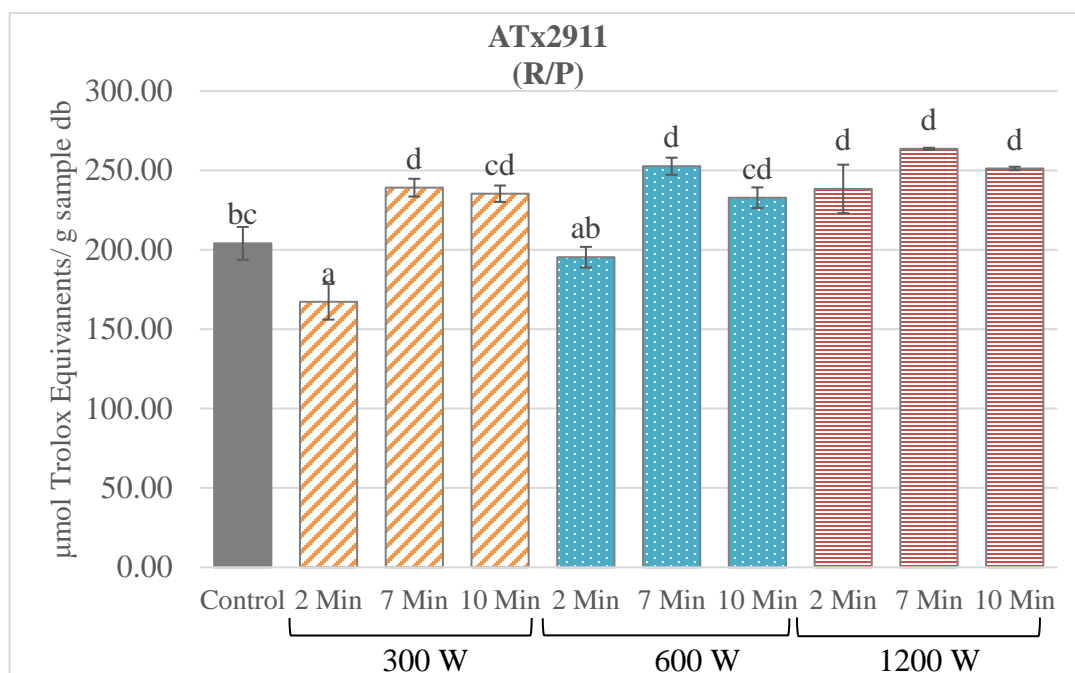


**Figure 22. Antioxidant capacity measured by trolox equivalents (TE) for control and MAE treated ATx2911 sorghum bran. Error bars = ± Standard Deviation (n=3) \*a-c: denotes statistical significance (p<0.05)**

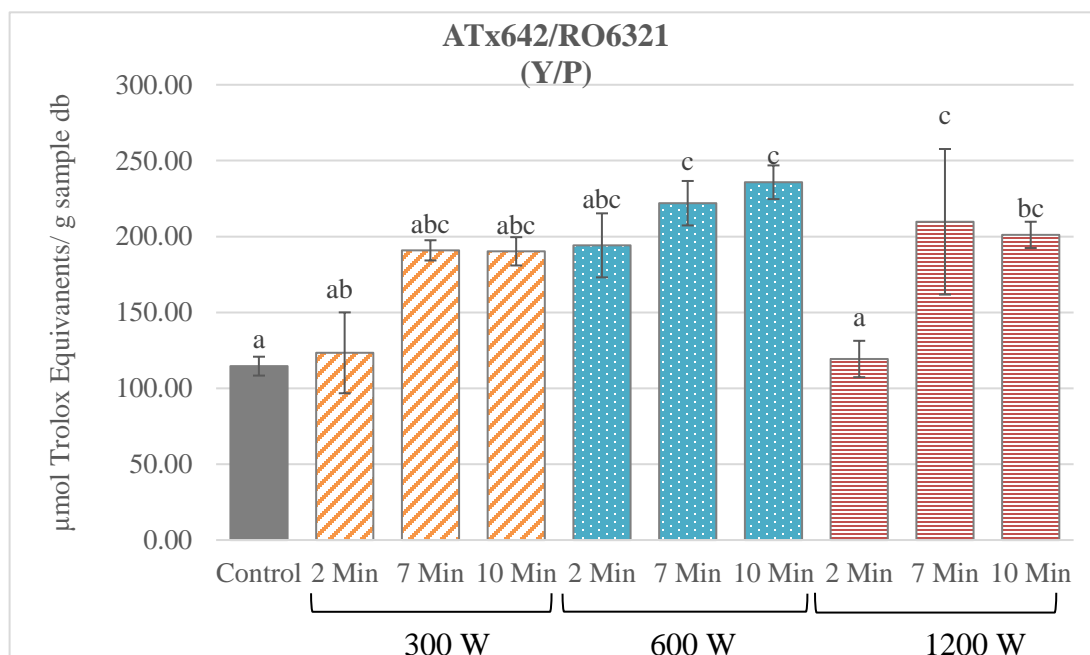


**Figure 23. Antioxidant capacity measured by trolox equivalents (TE) for control and MAE treated ATx642/RO6321 sorghum bran. Error bars = ± Standard Deviation (n=3) \*a-c: denotes statistical significance (p<0.05)**

## **Conclusion**

MAE had profound effects on the total extractable phenolics and antioxidant capacity of the phenotypes tested in this study. The W/T and W/P phenotypes showed the greatest increase in total extractable phenols and antioxidant capacity, with the R/T phenotype following close behind. The R/P phenotype showed no change in total phenolics while showing the least increase in antioxidant capacity. The Y/P phenotype showed no increase in total phenolics but a significant increase in antioxidant capacity.

The use of MAE has many different implications. The phenotype of the sorghum plays a large role in the outcome of MAE. White pericarp and high tannin sorghums benefit from MAE in terms of increasing antioxidant capacity and total phenolic content as a result of increased phenolic acid content. Pigmented sorghums, such as the R/P or Y/P phenotypes used in this study, had no great increase in phenolic content or antioxidant capacity. Phenolic extraction through MAE could still be beneficial with these types of sorghums as MAE was still able to extract an equivalent phenolic content and produced a slightly higher antioxidant capacity than the control extraction method.

## CHAPTER VI

### CONCLUSIONS

Sorghum grain is a source of many unique bioactive compounds concentrated in the bran. Understanding how microwave assisted extraction changes the polyphenolic profile from different phenotypes of sorghum grain can help clarify the most efficient ways to obtain the compounds for different applications.

Pericarp and secondary plant color influenced the changes in phenolic profile due to MAE. White pericarp sorghums had increases in phenolic content quantified by UPLC (1.6-11X versus control), as well as large increases in the folin phenolic content (3.4-3.5X) and antioxidant capacity (3.4-3.6X) after MAE. Pigmented pericarps with pigmented secondary plant color experienced a large decrease in the UPLC quantified phenolic content (50% of control) but little to no change in folin phenolic content quantified by the Folin-Ciocalteu test (1.1-1.2X increase versus control) following MAE treatment. The tannin phenotype showed increases in quantified phenolic content (5.0X versus control), total phenolic content (3.8X), and antioxidant capacity (3.5X) following MAE.

The increases in quantified phenolic contents, and antioxidant capacity of the white phenotypes was due to the breakdown of the cell wall material and release of the bound phenolic acids, mostly feruloyl-rhamnosides, under MAE. In the phenotype with red pericarp with purple secondary plant color, the losses in quantified phenolic content were primarily due to the degradation of free phenolic acids under MAE. The reduction

in phenolic content for the phenotype with lemon yellow pericarp and purple secondary plant color under MAE was mostly due to the degradation of flavanones (34% of control). This suggests that the specific structural features of polyphenolics affects their stability under microwave energy.

The tannin rich phenotype (red pericarp with tan secondary plant color) saw significant increases in phenolic acid content (5.0X versus control) and antioxidant capacity (3.5X), while anthocyanidins were detected after MAE treatment. The breakdown of the condensed tannins under MAE through oxidative depolymerization resulted in a release of monomeric flavonoids and their conversion to anthocyanidins which contributed to this increase. The consequences of the anthocyanidins on the functional properties of the tannin sorghum extracts should be investigated.

Depending on the compounds of interest, MAE can be utilized to extract higher amounts of specific classes of phenolics from a chosen sorghum phenotype, or even compounds that are not otherwise accessible without MAE (bound phenolic acids such as feruloyl-rhamnosides). However, MAE is not without its shortcomings. Some bioactive compounds, particularly free phenolic acids, flavanone-glycosides, and tannins are susceptible to rapid degradation under MAE conditions. Compound stability to MAE should be considered when using MAE to extract for specific compounds. Despite this, MAE is potentially a viable tool to efficiently extract polyphenolic compounds from sorghum bran.

Future work in this area to further understand the impact of tannins on the phenolic content, and structures of phenolic compounds following MAE would be

worthwhile. The impact of MAE on other sorghum phenotypes and biomass should also be explored to further identify the most efficient use of MAE to extract these valuable compounds.

## REFERENCES

- Agah, S., Kim, H., Mertens-Talcott, S.U., Awika, J.M., 2017. Complementary cereals and legumes for health: Synergistic interaction of sorghum flavones and cowpea flavonols against LPS-induced inflammation in colonic myofibroblasts. *Mol. Nutr. Food Res.* 61, 1600625. <https://doi.org/10.1002/mnfr.201600625>
- Aliaño-González, M.J., Espada-Bellido, E., Ferreiro-González, M., Carrera, C., Palma, M., Ayuso, J., Álvarez, J.Á., Barbero, G.F., 2020. Extraction of anthocyanins and total phenolic compounds from Açai (*Euterpe oleracea* Mart.) using an experimental design methodology. Part 2: Ultrasound-assisted extraction. *Agronomy* 10. <https://doi.org/10.3390/agronomy10030326>
- Anunciação, P.C., Cardoso, L. de M., Queiroz, V.A.V., de Menezes, C.B., de Carvalho, C.W.P., Pinheiro-Sant'Ana, H.M., Alfenas, R. de C.G., 2018. Consumption of a drink containing extruded sorghum reduces glycaemic response of the subsequent meal. *Eur. J. Nutr.* 57, 251–257. <https://doi.org/10.1007/s00394-016-1314-x>
- Awika, J.M., 2014. Sorghum: Its Unique Nutritional and Health-Promoting Attributes, Gluten-Free Ancient Grains. Elsevier Ltd. <https://doi.org/10.1016/B978-0-08-100866-9/00003-0>
- Awika, J.M., 2011. Major Cereal Grains Production and Use around the World.
- Awika, J.M., 2003. Antioxidant Properties of Sorghum.
- Awika, J.M., McDonough, C.M., Rooney, L.W., 2005a. Decorticating sorghum to concentrate healthy phytochemicals. *J. Agric. Food Chem.* 53, 6230–6234.



<https://doi.org/10.1021/jf0510384>

Awika, J.M., Rooney, L.W., Waniska, R.D., 2005b. Anthocyanins from black sorghum and their antioxidant properties. *Food Chem.* 90, 293–301.

<https://doi.org/10.1016/j.foodchem.2004.03.058>

Awika, J.M., Rose, D.J., Simsek, S., 2018. Complementary effects of cereal and pulse polyphenols and dietary fiber on chronic inflammation and gut health. *Food Funct.* 9, 1389–1409. <https://doi.org/10.1039/C7FO02011B>

Barros, F., Dykes, L., Awika, J., Rooney, L.W., 2013. Accelerated solvent extraction of phenolic compounds from sorghum brans. *J. Cereal Sci.* 58, 305–312.

<https://doi.org/10.1016/j.jcs.2013.05.011>

Beehmohun, V., Fliniaux, O., Grand, E., Lamblin, F., Bensaddek, L., Christen, P., Kovensky, J., Fliniaux, M.-A., Mesnard, F., 2007. Microwave-assisted Extraction of the Main Phenolic Compounds in Flaxseed. *Phytochem. Anal.* 275–282.

<https://doi.org/10.1002/pca.973>

Borden, D., 2011. Effect of Harvest Dates on Biomass Accumulation and Composition in Bioenergy Sorghum Effect of Harvest Dates on Biomass Accumulation and Composition in Bioenergy Sorghum.

C.F. Earp, J.O.A.S.H.R. and L.W.R., 1981. Evaluation of several methods to determine tannins in sorghums with varying kernel characteristics. *Cereal Chem.*

Chiremba, C., Rooney, L.W., Beta, T., 2012a. Microwave-Assisted Extraction of Bound Phenolic Acids in Bran and Flour Fractions from Sorghum and Maize Cultivars Varying in Hardness. <https://doi.org/10.1021/jf300279t>

- Chiremba, C., Taylor, J.R.N., Rooney, L.W., Beta, T., 2012b. Phenolic acid content of sorghum and maize cultivars varying in hardness. *Food Chem.* 134, 81–88.  
<https://doi.org/10.1016/j.foodchem.2012.02.067>
- Combs, C.A., 2016. *Tannins : Biochemistry, Food Sources and Nutritional Properties.* Nova Science Publishers, New York, NY.
- Dia, V.P., Pangloli, P., Jones, L., McClure, A., Patel, A., 2016. Phytochemical concentrations and biological activities of: *Sorghum bicolor* alcoholic extracts. *Food Funct.* 7, 3410–3420. <https://doi.org/10.1039/c6fo00757k>
- Dykes, L., 2008. *Flavonoid Composition and Antioxidant Activity of Pigmented Sorghums of Varying Genotypes.*
- Dykes, L., Peterson, G.C., Rooney, W.L., Rooney, L.W., 2011. Flavonoid composition of lemon-yellow sorghum genotypes. *Food Chem.*  
<https://doi.org/10.1016/j.foodchem.2011.03.020>
- Dykes, L., Rooney, L.W., 2007. Phenolic compounds in cereal grains and their health benefits. *Cereal Foods World* 52, 105–111.
- Dykes, L., Rooney, L.W., 2006. Sorghum and millet phenols and antioxidants. *J. Cereal Sci.* 44, 236–251. <https://doi.org/10.1016/J.JCS.2006.06.007>
- Dykes, L., Rooney, L.W., Waniska, R.D., Rooney, W.L., 2005. Phenolic Compounds and Antioxidant Activity of Sorghum Grains of Varying Genotypes. *J. Agric. Food Chem.* 53, 6813–6818. <https://doi.org/10.1021/jf050419e>
- Dykes, L., Seitz, L.M., Rooney, W.L., Rooney, L.W., 2009. Flavonoid composition of red sorghum genotypes. *Food Chem.* 116, 313–317.

<https://doi.org/10.1016/j.foodchem.2009.02.052>

Girard, A.L., Awika, J.M., 2018. Sorghum polyphenols and other bioactive components as functional and health promoting food ingredients. *J. Cereal Sci.* 84, 112–124.

<https://doi.org/10.1016/j.jcs.2018.10.009>

Gujer, R., Magnolato, D., Self, R., 1986. Glucosylated flavonoids and other phenolic compounds from sorghum. *Phytochemistry* 25, 1431–1436.

[https://doi.org/10.1016/S0031-9422\(00\)81304-7](https://doi.org/10.1016/S0031-9422(00)81304-7)

Herrman, D., 2016. Improvement of extractability and aqueous stability of sorghum 3-deoxyanthocyanins. *Food Sci. Technol.*

Herrman, D.A., Brantsen, J.F., Ravisankar, S., Lee, K.M., Awika, J.M., 2020. Stability of 3-deoxyanthocyanin pigment structure relative to anthocyanins from grains under microwave assisted extraction. *Food Chem.* 333, 127494.

<https://doi.org/10.1016/j.foodchem.2020.127494>

Kaderides, K., Papaoikonomou, L., Serafim, M., Goula, A.M., 2019. Microwave-assisted extraction of phenolics from pomegranate peels: Optimization, kinetics, and comparison with ultrasounds extraction. *Chem. Eng. Process. - Process Intensif.* 137, 1–11. <https://doi.org/10.1016/j.cep.2019.01.006>

Kaluza, W.Z., McGrath, R.M., Roberts, T.C., Schroder, H.H., 1980. Separation of Phenolics of Sorghum Bicolor (L.) Moench Grain. *J. Agric. Food Chem.* 28, 1191–1196. <https://doi.org/10.1021/jf60232a039>

Kang, J., Price, W.E., Ashton, J., Tapsell, L.C., Johnson, S., 2016. Identification and characterization of phenolic compounds in hydromethanolic extracts of sorghum

- wholegrains by LC-ESI-MSn. *Food Chem.* 211, 215–226.  
<https://doi.org/10.1016/j.foodchem.2016.05.052>
- Khan, I., Yousif, A.M., Johnson, S.K., Gamlath, S., 2015. Acute effect of sorghum flour-containing pasta on plasma total polyphenols, antioxidant capacity and oxidative stress markers in healthy subjects: A randomised controlled trial. *Clin. Nutr.* 34, 415–421. <https://doi.org/10.1016/j.clnu.2014.08.005>
- Li, Y., Guo, B., Wang, W., Li, L., Cao, L., Yang, C., Liu, J., Liang, Q., Chen, J., Wu, S., Zhang, L., 2019. Characterization of phenolic compounds from *Phyllanthus emblica* fruits using HPLC-ESI-TOF-MS as affected by an optimized microwave-assisted extraction. *Int. J. Food Prop.* 22, 330–342.  
<https://doi.org/10.1080/10942912.2019.1583249>
- Links, M.R., Taylor, J., Kruger, M.C., Naidoo, V., Taylor, J.R.N., 2016. Kafirin microparticle encapsulated sorghum condensed tannins exhibit potential as an anti-hyperglycaemic agent in a small animal model. *J. Funct. Foods* 20, 394–399.  
<https://doi.org/10.1016/j.jff.2015.11.015>
- Links, M.R., Taylor, J., Kruger, M.C., Taylor, J.R.N., 2015. Sorghum condensed tannins encapsulated in kafirin microparticles as a nutraceutical for inhibition of amylases during digestion to attenuate hyperglycaemia. *J. Funct. Foods* 12, 55–63.  
<https://doi.org/10.1016/j.jff.2014.11.003>
- Lopes, R. de C.S.O., de Lima, S.L.S., da Silva, B.P., Toledo, R.C.L., Moreira, M.E. de C., Anunciação, P.C., Walter, E.H.M., Carvalho, C.W.P., Queiroz, V.A.V., Ribeiro, A.Q., Martino, H.S.D., 2018. Evaluation of the health benefits of consumption of

extruded tannin sorghum with unfermented probiotic milk in individuals with chronic kidney disease. *Food Res. Int.* 107, 629–638.

<https://doi.org/10.1016/j.foodres.2018.03.004>

Malunga, L.N., Beta, T., 2016. Isolation and identification of feruloylated arabinoxylan mono- and oligosaccharides from undigested and digested maize and wheat.

*Heliyon* 2. <https://doi.org/10.1016/j.heliyon.2016.e00106>

Mateo Anson, N., Aura, A., Selinheimo, E., Mattila, I., Poutanen, K., van den Berg, R., Havenaar, R., Bast, A., Haenen, G.R.M.M., 2011. Bioprocessing of Wheat Bran in Whole Wheat Bread Increases the Bioavailability of Phenolic Acids in Men and Exerts Antiinflammatory Effects ex Vivo. *J. Nutr.* 141, 137–143.

<https://doi.org/10.3945/jn.110.127720>

Mazza, G., Brouillard, R., 1987. Color Stability and Structural Transformations of Cyanidin 3,5-Diglucoside and Four 3-Deoxyanthocyanins in Aqueous Solutions. *J. Agric. Food Chem.* 35, 422–426. <https://doi.org/10.1021/jf00075a034>

Ojwang, L., Awika, J.M., 2008. Effect of phytate and storage conditions on the development of the ‘ hard-to-cook .’ *J. Sci. Food Agric.* 88, 1987–1996.

<https://doi.org/10.1002/jsfa>

Ojwang, L.O., Dykes, L., Awika, J.M., 2012. Ultra performance liquid chromatography-tandem quadrupole mass spectrometry profiling of anthocyanins and flavonols in cowpea (*Vigna unguiculata*) of varying genotypes. *J. Agric. Food Chem.* 60, 3735–3744. <https://doi.org/10.1021/jf2052948>

Pal, C.B.T., Jadeja, G.C., 2020. Microwave-assisted extraction for recovery of

polyphenolic antioxidants from ripe mango (*Mangifera indica* L.) peel using lactic acid/sodium acetate deep eutectic mixtures. *Food Sci. Technol. Int.* 26, 78–92.

<https://doi.org/10.1177/1082013219870010>

Pale, E., Kouda-Bonafos, M., Nacro, M., Vanhaelen, M., Vanhaelen-Fastré, R., Ottinger, R., 1997. 7-O-methylapigeninidin, an anthocyanidin from *Sorghum caudatum*.

*Phytochemistry* 45, 1091–1092. [https://doi.org/10.1016/S0031-9422\(97\)00099-X](https://doi.org/10.1016/S0031-9422(97)00099-X)

Pham, L., Quoc, T., 2020. Microwave-Assisted Extraction of Phenolic Compounds From Ginger (*Zingiber Officinale* Rosc.). *Carpathian J. Food Sci. Technol.*

<https://doi.org/10.34302/crpjfst/2020.12.1.16>

Przybylska-Balcerek, A., Frankowski, J., Stuper-Szablewska, K., 2019. Bioactive compounds in sorghum. *Eur. Food Res. Technol.* 245, 1075–1080.

<https://doi.org/10.1007/s00217-018-3207-0>

Quiles-Carrillo, L., Mellinas, C., Garrigos, M.C., Balart, R., Torres-Giner, S., 2019.

Optimization of Microwave-Assisted Extraction of Phenolic Compounds with Antioxidant Activity from Carob Pods. *Food Anal. Methods* 12, 2480–2490.

<https://doi.org/10.1007/s12161-019-01596-3>

Rahmani, Z., Khodaiyan, F., Kazemi, M., Sharifan, A., 2020. Optimization of microwave-assisted extraction and structural characterization of pectin from sweet lemon peel. *Int. J. Biol. Macromol.* 147, 1107–1115.

<https://doi.org/10.1016/j.ijbiomac.2019.10.079>

Ravisankar, S., 2019. Interactive Effects of Cereal-pulse Flavonoid combinations on their Bioavailability. <https://doi.org/10.1017/CBO9781107415324.004>

- Ravisankar, S., Abegaz, K., Awika, J.M., 2018. Structural profile of soluble and bound phenolic compounds in teff (*Eragrostis tef*) reveals abundance of distinctly different flavones in white and brown varieties. *Food Chem.* 263, 265–274.  
<https://doi.org/10.1016/j.foodchem.2018.05.002>
- Simnadis, T.G., Tapsell, L.C., Beck, E.J., 2016. Effect of sorghum consumption on health outcomes: A systematic review. *Nutr. Rev.* 74, 690–707.  
<https://doi.org/10.1093/nutrit/nuw036>
- Stefoska-Needham, A., Beck, E.J., Johnson, S.K., Batterham, M.J., Grant, R., Ashton, J., Tapsell, L.C., 2017. A Diet Enriched with Red Sorghum Flaked Biscuits, Compared to a Diet Containing White Wheat Flaked Biscuits, Does Not Enhance the Effectiveness of an Energy-Restricted Meal Plan in Overweight and Mildly Obese Adults. *J. Am. Coll. Nutr.* 36, 184–192.  
<https://doi.org/10.1080/07315724.2016.1237314>
- Stefoska-Needham, A., Beck, E.J., Johnson, S.K., Chu, J., Tapsell, L.C., 2016. Flaked sorghum biscuits increase postprandial GLP-1 and GIP levels and extend subjective satiety in healthy subjects. *Mol. Nutr. Food Res.* 60, 1118–1128.  
<https://doi.org/10.1002/mnfr.201500672>
- Svensson, L., Sekwati-Monang, B., Lutz, D.L., Schieber, R., Gänzle, M.G., 2010. Phenolic acids and flavonoids in nonfermented and fermented red sorghum (*Sorghum bicolor* (L.) Moench). *J. Agric. Food Chem.* 58, 9214–9220.  
<https://doi.org/10.1021/jf101504v>
- Sweeny, J.G., Iacobucci, G.A., 1983. Effect of Substitution on the Stability of 3-

- Deoxyanthocyanidins in Aqueous Solutions. *J. Agric. Food Chem.* 31, 531–533.  
<https://doi.org/10.1021/jf00117a017>
- Teferra, T.F., Amoako, D.B., Rooney, W.L., Awika, J.M., 2019. Qualitative assessment of ‘highly digestible’ protein mutation in hard endosperm sorghum and its functional properties. *Food Chem.* 271, 561–569.  
<https://doi.org/10.1016/j.foodchem.2018.08.014>
- USDA, U.S.D. of A., 2019. World Agricultural Production. *Circ. Ser.* 6–15.
- Wu, Yuye, Li, X., Xiang, W., Zhu, C., Lin, Z., Wu, Yun, Li, J., Pandravada, S., Ridder, D.D., Bai, G., Wang, M.L., Trick, H.N., Beane, S.R., Tuinstra, M.R., Tesso, T.T., Yu, J., 2012. Presence of tannins in sorghum grains is conditioned by different natural alleles of Tannin1. *Proc. Natl. Acad. Sci. U. S. A.* 109, 10281–10286.  
<https://doi.org/10.1073/pnas.1201700109>
- Xiong, Y., Zhang, P., Warner, R.D., Fang, Z., 2019. Sorghum Grain: From Genotype, Nutrition, and Phenolic Profile to Its Health Benefits and Food Applications. *Compr. Rev. Food Sci. Food Saf.* 18, 2025–2046. <https://doi.org/10.1111/1541-4337.12506>
- Yang, L., 2009. Chemopreventive Potential of Sorghum With Different Phenolic Profiles.
- Yang, L., Allred, C.D., Awika, J.M., 2014. Emerging evidence on the role of estrogenic sorghum flavonoid in colon cancer prevention. *Cereal Foods World* 59, 244–251.  
<https://doi.org/10.1094/CFW-59-5-0244>
- Yang, L., Allred, K.F., Dykes, L., Allred, C.D., Awika, J.M., 2015. Enhanced action of



apigenin and naringenin combination on estrogen receptor activation in non-malignant colonocytes: Implications on sorghum-derived phytoestrogens. *Food Funct.* 6, 749–755. <https://doi.org/10.1039/c4fo00300d>

Yang, L., Allred, K.F., Geera, B., Allred, C.D., Awika, J.M., 2012. Sorghum phenolics demonstrate estrogenic action and induce apoptosis in nonmalignant colonocytes. *Nutr. Cancer* 64, 419–427. <https://doi.org/10.1080/01635581.2012.657333>

Yang, Liyi, Dykes, L., Awika, J.M., 2014. Thermal stability of 3-deoxyanthocyanidin pigments. *Food Chem.* 160, 246–254. <https://doi.org/10.1016/j.foodchem.2014.03.105>

Zhao, Z., Dahlberg, J., 2019. *Sorghum Methods and Protocols.*